https://doi.org/10.5194/egusphere-2026-4943
Preprint. Discussion started: 28 September 2026

Coupling Tree-Ring Blue Intensity and Carbon Isotope ($\delta^{13}C$) Reveals Shifting Climate Change Drivers on Tree Growth in Kurdistan Forests, Northern Iraq

Khalat F. Mohammed[1,4], Philippe Claeys[2,3], Kamal Kolo[1,4]

1. Climate Change and Sustainability Research Centre, Soran University, Soran, 44008, Kurdistan Region, IRAQ
2. Archaeology, Environmental Changes & Geo-Chemistry, Vrije Universiteit Brussel, Pleinlaan 2, 1050 Brussel, Belgium
3. Pacific Centre for Isotope and Geochemical Research, Dept. Earth, Ocean and Atmospheric Sciences, University of British Columbia, Vancouver, BC, V6T 1Z4 (2329 West Mall), Canada
4. Department of Petroleum Geoscience, Soran University, Soran, 44008, Kurdistan Region, IRAQ

Correspondence to: khalat F. Mohammed (khalat.mohammed@soran.edu.iq.com)

Abstract. This study investigates the relationships between climate changes and growth in semi-arid forests located in the Kurdistan Region of northern Iraq by utilizing tree-ring Blue Intensity (BI) parameters alongside stable carbon isotopes ($\delta^{13}C$). The sensitivity of detrended tree-ring width (TRW), earlywood blue intensity (EWBI), latewood blue intensity (LWBI), and delta blue intensity ΔBI to temperature, precipitation, and physiological responses are measured on three species of tree *Quercus aegilops*, *Juglans regia* and *Fraxinus*. Tree-ring Blue Intensity chronologies for 100 years, are used to look at climate-growth interactions over time for all three species. Results show a dominant temperature control on wood formation. EWBI is correlates with temperature ($r \approx 0.37$, $p < 0.001$) and with precipitation in *Quercus aegilops*, whereas ΔBI is a positive temperature proxy ($r \approx 0.37$, $p < 0.001$), this shows that when years are warmer, the density contrast of earlywood and latewood is increased. In Juglans regia, the strongest temperature sensitivity in TRW is found in LWBI ($r \approx -0.45$, $p < 0.001$). The positive correlation of ΔBI with $\delta^{13}C$ ($r \approx 0.30$, $p < 0.01$) indicates a positive structural and physiological response to drought stress. The TRW sensitivities of Fraxinus are weaker ($r = 0.128$ in Erbil, $r = 0.122$ in Duhok), and the temperature BI(EW-LW) relationships are negative and significant ($r \approx -0.340$, $p < 0.01$) ($r \approx -0.280$, $p < 0.01$). Wavelet coherence analysis indicates a shift in the growth trend from precipitation-driven growth prior to ~1980 to the temperature-related growth thereafter, with increasing non-stationarity and episodic drought signatures. The integrated BI-$\delta^{13}C$ approach captures anatomical and physiological adjustment, revealing that recent warming led to a decrease in radial growth, less earlywood development and changed wood density structure across species. The results show the potential of BI as an effective indicator of detecting climate-driven ecosystem shifts and temperature variability.

https://doi.org/10.5194/egusphere-2026-4943
Preprint. Discussion started: 28 September 2026

1 Introduction

Climate change is increasingly compromising the ability of forests to function as carbon sinks due to changes in temperature and precipitation, affecting the structure and function of forest ecosystems (Barbosa and Asner, 2016). This phenomenon influences tree metabolism by altering photosynthesis and respiration rates (Breshears et al., 2021, Scafaro et al., 2021). The impact of climate change is broader and more severe than earlier evaluations suggested (Lee et al., 2023). Understanding current and future climate dynamics necessitates a comprehensive assessment of past climatic variability (Solomon, 2007). Tree-Ring (TR) data, serving as a high-resolution proxy for long-term environmental monitoring, enables reconstruction of climatic variations over hundreds (Cook et al., 2013, Heeter et al., 2021, Shah et al., 2023) to thousands of years (Wilson et al., 2016). Such data offer crucial details regarding the magnitudes of climatic fluctuations that occur naturally and last longer than the observational period. While proxies for reconstructing precipitation, drought, and other climate variables are common, temperature-sensitive proxies remain rare (Mann et al., 2008, Christiansen and Ljungqvist, 2017, Macdonald, 2020). Dendroclimatology indicates that trees at high-elevation or latitude tree lines are primarily temperature-limited, while at lower altitudes or latitudes, moisture limitations dominate growth (Kienast et al., 1987, Briffa et al., 2002, George, 2014). Reliable reconstructions depend on effective sampling within tree-line locations governed mainly by a single climate parameter (Bradley, 1999).

Research utilizing tree-rings for historical climate reconstruction, particularly temperature, has been well-documented (Eschbach et al., 1995, D'Arrigo et al., 2006, Buckley et al., 2018). The technique of X-ray densitometry, which measures the Maximum Latewood Density (MXD), was prominent until the early 21st century (Eschbach et al., 1995) and became important in the 1980s for enhancing the Northern Hemisphere's temperature-sensitive tree ring records (Schweingruber et al., 1978). However, recent developments include Blue Intensity (BI) analysis, a cost-effective alternative gaining traction in dendroclimatological studies (McCarroll et al., 2002, Campbell et al., 2007, Kaczka et al., 2018, Kaczka and Wilson, 2021, Cao et al., 2022). BI measures the intensity of blue light reflected from wood surfaces (Kaczka et al., 2018). The wood's optical characteristics influence the BI value, linked to the lignin content in latewood cell walls according to McCarroll et al. (2002) and Campbell et al. (2007), with results reflecting latewood cell wall lignin content, as lignin absorbs UV light more readily than other components (Fukazawa, 1992). High BI values correlate with lower wood density and vice versa (Björklund et al., 2021, Björklund et al., 2024), with BI demonstrating efficacy in indicating summer temperatures despite RW's weaknesses at lower latitudes (Heeter et al., 2020, Zheng et al., 2023).

The increasing number of studies utilizing BI for summer temperature reconstruction emphasizes its validity as a substitute for MXD, particularly when large-scale temperature reconstructions are required in inaccessible areas (Wilson et al., 2014, Wilson et al., 2019, Buckley et al., 2018, Fuentes et al., 2018, Heeter et al., 2021). Numerous experimental studies demonstrated a strong correlation between BI and MXD (Campbell et al., 2007, Campbell et al., 2011, Björklund et al., 2014, Björklund et al., 2015). Moreover, monitoring physiological and ecological responses of various tree species offers insights into their reactions to climate change (Marchand et al., 2020), particularly through intrinsic Water-use Efficiency (iWUE),

https://doi.org/10.5194/egusphere-2026-4943
Preprint. Discussion started: 28 September 2026

crucial for tree growth evaluation (Churakova et al., 2020). C_3 trees are especially sensitive to moisture variability, recording hydroclimatic changes through radial growth and carbon isotope signatures and providing valuable paleoclimate indicators as trees normally discriminate strongly against $^{13}CO_2$ during photosynthesis, preferring the lighter $^{12}CO_2$ (Cernusak et al., 2013). Drought stress reduces isotope discrimination in these trees, producing $\delta^{13}C$ values that serve as proxies for historical water stress intensity, crucial for paleoclimate reconstruction and drought monitoring studies (Diefendorf et al., 2010, Kohn, 2010). Stable isotope measurements from tree-rings are significant for understanding historical environmental changes and the global carbon cycle (Wilson and Grinsted, 1977), as stable carbon isotopes respond variably across species and regions (Francey and Farquhar, 1982). A number of investigations have created climate reconstructions using whole-wood stable isotopes measurements (Verheyden et al., 2005, Harlow et al., 2006). Tree-ring and $\delta^{13}C$ data from various coniferous and broadleaf tree species have been used to accurately reconstruct climate data spanning hundreds to thousands of years across many regions (Saurer and Siegenthaler, 1989, Saurer et al., 1995, Pawelczyk et al., 2004, Hafner and Levanič, 2009). The study investigates the combined impact of blue intensity parameters and stable carbon isotopes ($\delta^{13}C$) on temperature and precipitation variations in Kurdistan forests. It aims to identify key climate variables influencing tree growth and assess trends over time, enhancing understanding of the non-stationarity in growth-climate relationships within semi-arid forest ecosystems.

2 Materials and Methods

2.1 Tree-Ring Data and Blue Intensity Processing

Two tree slabs from stump and one core sample were collected from various species and locations in the Kurdistan Region. The first example is a walnut tree *Juglans regia* (WSS-2) that was felled in 2024 and is located in Sidakan, Soran area (36°39'21.06 N 44°32'31.67 E). The second sample was obtained from oak tree (QASA) known as *Quercus aegilops* that had been felled in 2023 in the Alka Village, Barzan area (36°55'44.23 N 44°02'10.08 E). The third sample, a single increment core was taken from *Fraxinus* (commonly called Bnaw) in Kani Shakr, in the Mirgasur area (**Fig. 1**). The tree core was extracted using a Swedish Haglöf increment borer, available in lengths of 25 cm and 50 cm, with a diameter of 5.15 mm. This tool is commonly employed in dendrochronological and dendroclimatological studies. The double-helix screw thread design ensures efficient and smooth penetration into the tree trunk.

https://doi.org/10.5194/egusphere-2026-4943
Preprint. Discussion started: 28 September 2026

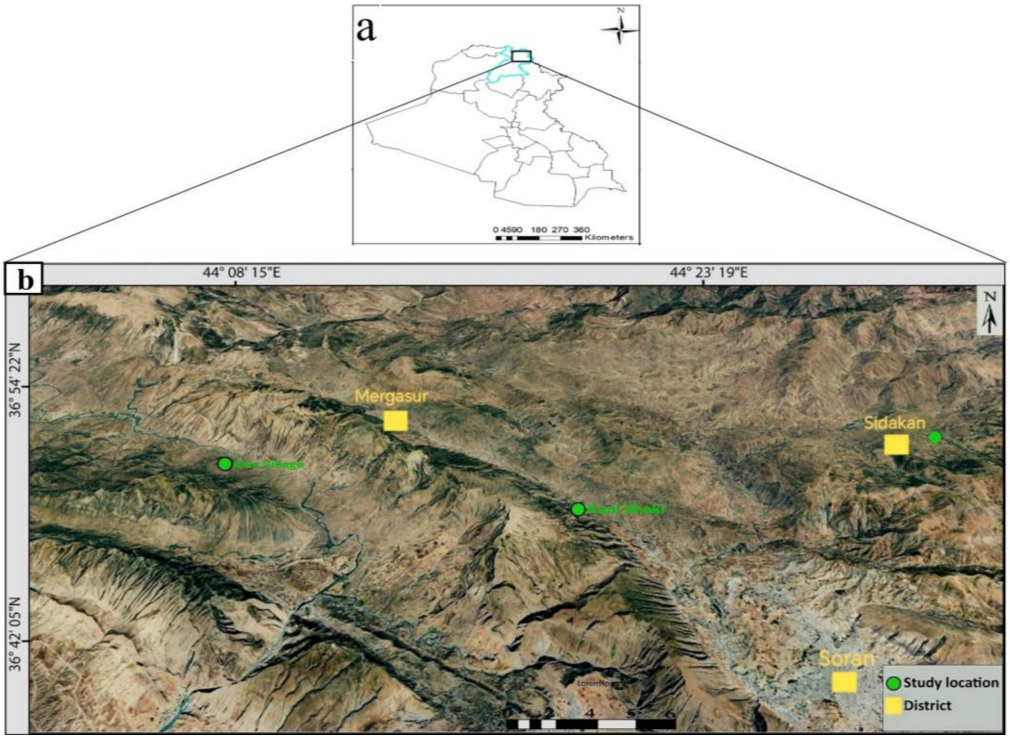

Figure 1: (a) general map of Iraq. (b) topographic image with green points, location of study areas.

Slabs and increment core were prepared for analysis using the standard methods outlined by Stokes (1996). The samples were left to air dry at least 24 hours. The tracheid cells were then set up in the vertical position by placing the core. After the samples had been dried and core mounted, each sample was sanded sequentially with the rotating belt sander, increasingly higher grit starting from 80 up to 800. The final polishing was performed manually using 1200 grit sandpaper if any obvious scratches or blemishes from mechanical sanding were present. This procedure was followed in order to have high resolution image scanning.

For tree-ring and blue Intensity measurement, core and slabs (**Fig. 2**) were scanned with a resolution of 1200 dots per inch (dpi) using the flatbed CanoScan LiDE 300. CooRecorder 9.8.1 software (Cybis Elektronik & Data AB) was used to load each scanned image separately for the purposes of measuring Tree-Ring Width (TRW) and analyzing (BI) (**Fig. 3**), and both manual and automatic placement were used to mark the ring boundaries (Maxwell and Larsson, 2021).

https://doi.org/10.5194/egusphere-2026-4943
Preprint. Discussion started: 28 September 2026

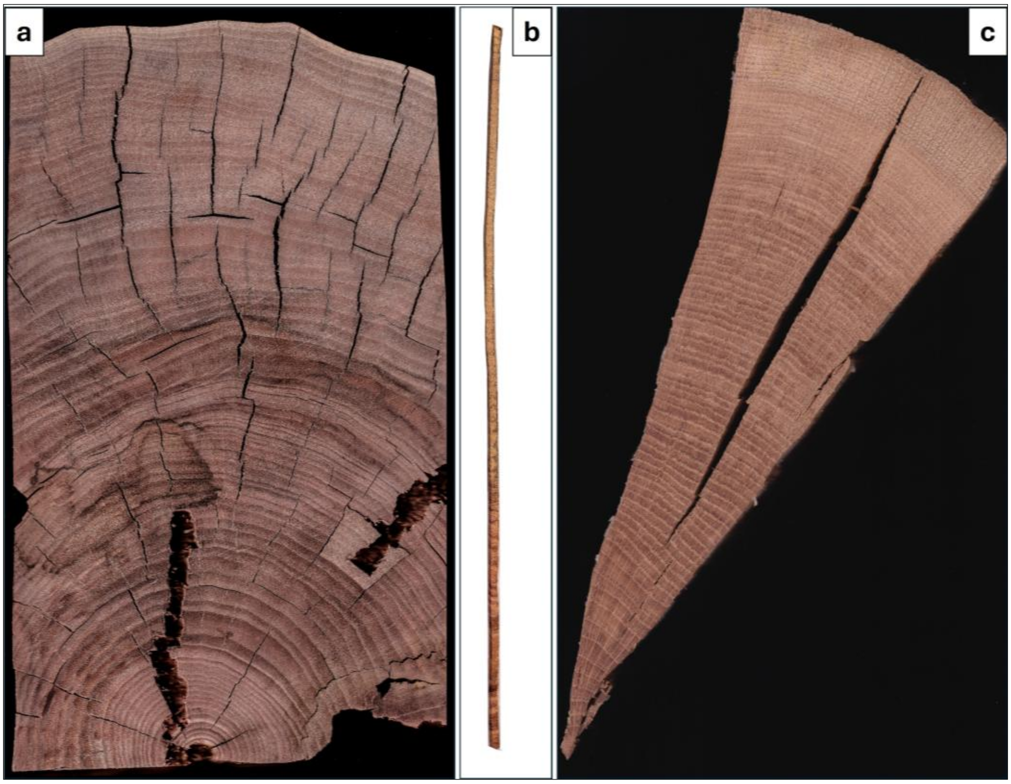

100 **Figure 2: Scanned slab and core samples with a resolution of 1200 dots per inch (dpi) by using the flatbed CanoScan LiDE 300. (a) Slab walnut sample (WSS2), (b) Core *Fraxinus* sample locally known as Bnaw, (c) Slab-cut oak sample (QASA). All were used for BI measurements.**

https://doi.org/10.5194/egusphere-2026-4943
Preprint. Discussion started: 28 September 2026

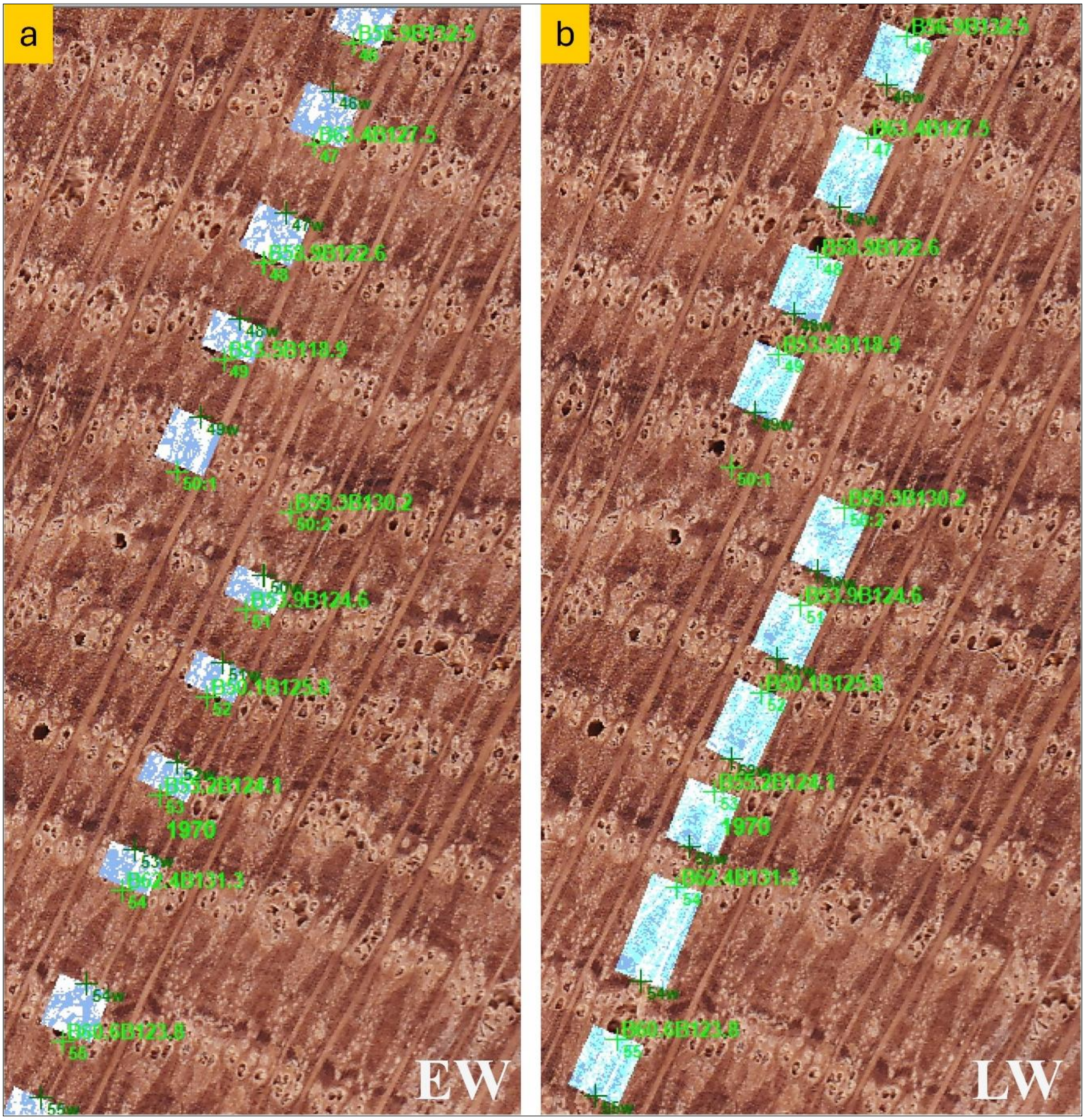

Figure 3: For every yearly ring, BI and RW measurements are gathered using CooRecorder 9.8.1 (Cybis Elektronik & Data AB) image analysis software. Code example (QASA). (a) the whitest 100% of pixels in the highlighted box are measured (dark blue) for Early Wood (EW) after all the pixels are sorted by light and dark wood (white and blue, respectively). Measurements for Late Wood (LW) (b) are obtained from 30% of the darkest pixels (dark blue). To calculate ΔBI, the LW measurements are obtained and subtracted from the EW measurement using a 100%-pixel average (for interpretation of the color references in this figure legend).

Each sample's individual growth rings were measured with an accuracy of 0.001 mm. For BI measurements, CooRecorder offers a number of data output options (**Fig. 4**).

https://doi.org/10.5194/egusphere-2026-4943
Preprint. Discussion started: 28 September 2026

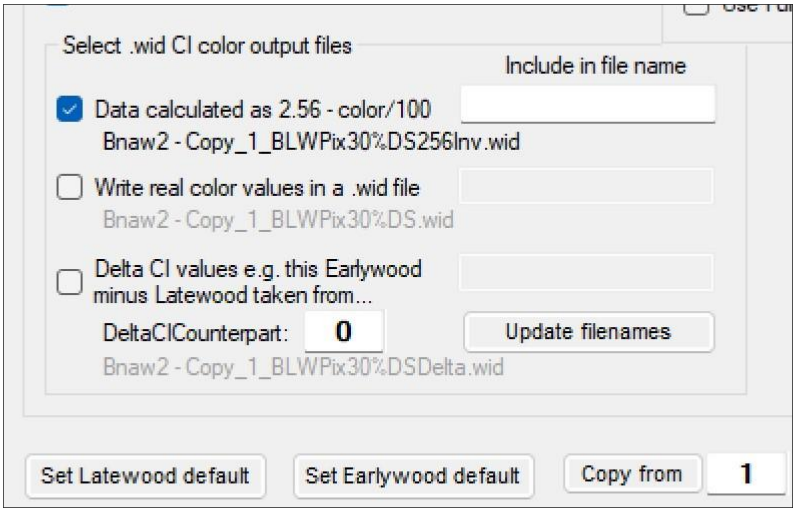

Figure 4: Screenshot displays available data of outputs from CooRecorder 9.8.1 (Cybis Elektronik & Data AB) software.

Delta Blue Intensity (ΔBI), Earlywood Blue Intensity (EWBI), and Late Wood Blue Intensity (LWBI) were inverted (Björklund et al., 2024) and data were generated. The reflectance value from a frame structure with user-defined frame specifications was recorded to calculate BI data concurrently with TRW (**Fig. 5**). For BI measurements, three samples were used. For WSS2, this study uses a relative margin (k) (0.30) to the next ring border for LWBI, a frame width of 100, a width-limiting factor of 3, a frame position of 5, and a maximum frame deepness of 200. In addition, the EWBI has a relative margin (k) (0.05) to the next ring border, a frame position of -2, a maximum frame deepness of 500, a frame width of 100, and a width-limiting factor of 3. For the second sample QASA, the frame width was set at 70, the width-limiting factor at 3, the frame position at 5, the maximum frame depth at 500, and the relative margin (k) to the next ring border for LWBI at 0.30. In addition, the EWBI has a relative margin (k 0.05) to the next ring border, a frame position of -2, a maximum frame deepness of 200, a frame width of 70, and a width-limiting factor of 3A frame width of 50, a width-limiting factor of 3, a frame position of 5, a maximum frame deepness of 500, and a relative margin (k) (0.30) to the next ring border for LWBI were all used. In this study for the third sample Bnaw, the EWBI has a relative margin (k 0.05) to the next ring border, a frame position of -2, a maximum frame deepness of 200, a frame width of 50, and a width-limiting factor of 3. These frame specifications are founded on the specifications applied by (Rydval et al., 2014). The values of percentile extraction are 85% and 15% percent which have been proven to deliver the best results in past researches (Rydval et al., 2014, Zheng et al., 2023), but in this case in all three samples, we used 100 %and 30 % to obtain the light and dark wood reflection intensity information of EWBI and LWBI. Negative exponential and heavy detrend were used in CDendro to detrend the RW measurements. The high-frequency climate signal is retained in this detrending process but all long-term trends that are not non-climate-induced trends are removed (Cook and Peters, 1981).

https://doi.org/10.5194/egusphere-2026-4943
Preprint. Discussion started: 28 September 2026

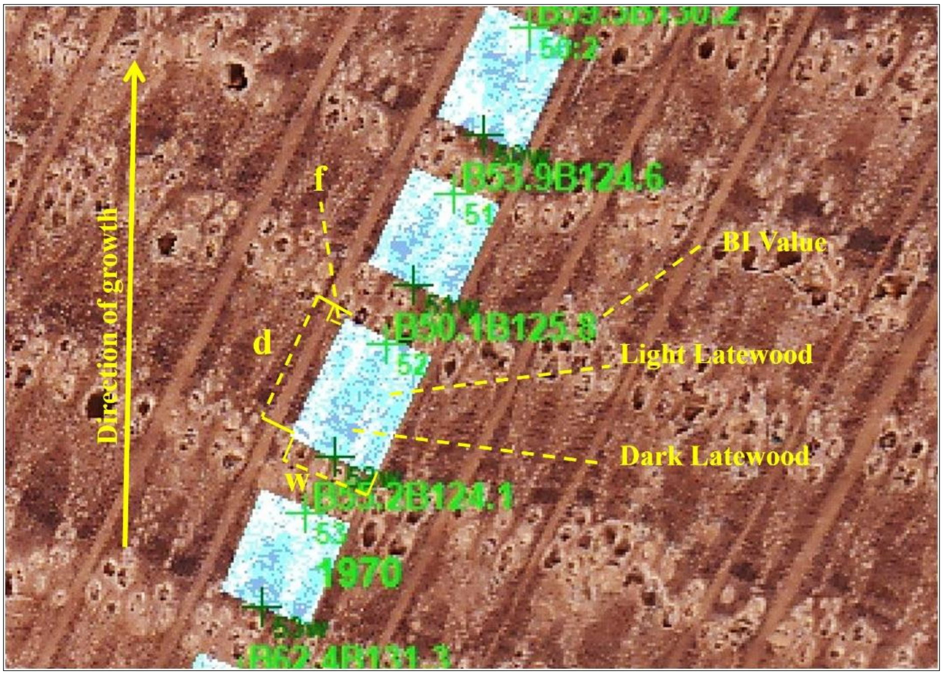

Figure 5: CooRecorder BI generation window with adjustable parameters (w, f, and d are measured in pixels): width, depth, and percentage of dark latewood. Code example (QASA).

2.2 Carbon Isotope Analysis ($\delta^{13}C$)

Carbon isotope analysis was conducted on wood samples by using an Elemental Analyzer (Eurovector EA3100) coupled to a Nu Horizon Isotope Ratio Mass Spectrometer (IRMS) for the measurement of $\delta^{13}C$ values. Calibration with reference material (e.g., IAEA-CH-6) was included periodically throughout the analytical sequence, at Archaeology, Environmental changes & Geo-Chemistry (AMGC), Vrije Universiteit Brussel.

A total of 98 wood samples were extracted from the WSS2 tree specimen along the radius from the pith to the bark, with each sample representing the material between consecutive annual rings for $\delta^{13}C$ analysis. All samples were manually ground to a fine homogeneous powder using a cleaned mortar. Strict clean environment and cleaning precaution procedures were applied between samples to ensure against any potential contamination. Approximately 3 mg of finely ground wood sample was weighed into tin capsules for $\delta^{13}C$ analysis. Prepared samples were stored in sealed containers prior to laboratory pretreatment and measurement. Since industrialization, changes in the concentration and stable isotopic composition of atmospheric CO2 have significantly affected the $\delta^{13}C$ of tree-ring cellulose through two primary mechanisms. The first mechanism involves the gradual depletion of $\delta^{13}C$ in atmospheric CO2 (referred to as $\delta^{13}C_{atm}$) primarily caused by fossil fuel combustion. This depletion is assimilated into tree-ring cellulose, resulting in a declining trend in tree-ring $\delta^{13}C$. It is important to note that this trend is not associated with physiological alterations in the trees or their responses to climate variations, a phenomenon commonly referred to as the Suess Effect. This effect is corrected using the standard dendro-isotopic practice of subtracting the change in

https://doi.org/10.5194/egusphere-2026-4943
Preprint. Discussion started: 28 September 2026

$\delta^{13}C_{atm}$ from each raw tree-ring $\delta^{13}C$ value, against a reference of -6.6‰, a value measured from a preindustrial sample of trees (McCarroll and Loader, 2004, Keeling et al., 2017, Belmecheri and Lavergne, 2020). This correction yields a $\delta^{13}C$ series, designated as ($\delta^{13}C$-corr), which, by eliminating the fossil fuel effect, more accurately represents natural environmental variations.

2.3 Historical Meteorological Data (Climate Data)

Long-term meteorological data were sourced from the World Bank Climate Data portal (*https://climateknowledgeportal.worldbank.org/country/iraq/climate-data-historical.org: accessed in June, 2025)*. Annual mean temperature and precipitation records were obtained from two stations, which are proximal to the study area: Erbil and Duhok. The data range is 1901-2024 offering a continuous record that can be used to carry out dendroclimatic studies.

2.4 Integrated Statistical Analysis

OriginPro 2022 (OriginLab Corporation, Northampton, MA, USA) was used for climate variables (temperature and precipitation) with DTRW, EWBI, LWBI, ΔBI, and $\delta^{13}C$ to conduct Correlation Coefficients and P-Value analyses.

2.5 Wavelet Coherence Analysis

All analyses of wavelet coherence maps were run on Windows 10 using the Anaconda Distribution (graphical installer downloaded from the official Anaconda website). After installation, Conda was initialized for PowerShell so that the conda command would be available in a new terminal session and verified the installation. To ensure reliable access to precompiled scientific and geospatial packages, configured Conda to use the conda-forge channel with strict channel priority. Then created an isolated Conda environment named pyleo, provisioned with Python 3.11 and Cartopy from conda-forge; Cartopy was installed via Conda as it depends on compiled libraries that are best obtained from conda-forge binaries. Inside that environment, was upgraded the Python packaging toolchain (pip, setup tools, wheel) and installed Pyleoclim via pip (Khider et al., 2022). The Pyleoclim release used here is distributed on PyPI and resolves cleanly once NumPy and SciPy are supplied by the environment. Successful installation was confirmed by importing Pyleoclim and recording its version (v1.2.1).

All computations were executed within the pyleo environment to guarantee reproducibility. In practice, it was either activated the environment (conda activate pyleo) and ran Python directly, or invoked Python non-interactively with conda run -n pyleo to avoid explicit activation within scripts. The input data were provided as CSV files, and a command-line Python script read the requested columns (e.g., tree-ring metrics and climate variables) and produced Continuous Wavelet Transforms (CWT) and R^2 Wavelet Coherence maps for each pair of variables of the dataset. This workflow - base Anaconda installation, environment creation on conda-forge with strict priority, cartopy via Conda, Pyleoclim via pip, and execution from the pyleo environment -prevented Windows compiler errors, pinned core dependencies, and provided a fully reproducible setup for our dendroclimatological analyses.

https://doi.org/10.5194/egusphere-2026-4943
Preprint. Discussion started: 28 September 2026

3 Results

3.1 Chronology Characteristics of Detrended TRW and BI Parameters with Climate and Physiological Signal

3.1.1 *Quercus Aegilops* (QASA)

Detrended TRW is negatively correlated (weakly but significantly) with mean temperature at Erbil (r = -208, p = 0.041) as well as Duhok (r = -216, p = 0.034, **Table 1**), but there is no significant effect of precipitation. It means that an increase in temperatures is connected to a decrease in radial growth even in the moderate to high rainfall years. The EWBI has the strongest BI sensitivity among BI parameters. It exhibits moderate negative and highly significant correlation with mean temperature (r = -0.37 in Erbil, r = -0.38 in Duhok, in both cases, p <0.001) and positive correlation with precipitation (r = 0.269, p = 0.0078 in Erbil; r = 0.250, p = 0.0138 in Duhok) (**Table 1**). The negative correlation of EWBI with $\delta^{13}C$, which is weak but significant (r = -0.223, p = 0.029, **Table 1**) is associated with the interpretation that increased EWBI value correlates with decreased $\delta^{13}C$, which means increased stomatal conductance and reduced intrinsic water-use efficiency in moist years. By contrast, LWBI does not respond to temperature, the correlation is near to zero, but has a weak positive correlation with precipitation in Erbil (r = 0.228, p = 0.025) (**Table 1**). This implies that the variability in hydroclimatic intensity only exerts a minor effect on latewood intensity, and its role in the climatic signal is secondary compared to EWBI and ΔBI. The ΔBI turns out to be a strong predictor of temperature variability as it has high positive correlations with mean temperature (r = 0.36 and r = 0.37, p < 0.001 in the case of Erbil and Duhok, respectively, **Table 1**). This shows that when years are warmer, the density contrast of earlywood and latewood increases. This observation is supported by the further positive, although weaker, relationship with $\delta^{13}C$, which is significant (r = 0.284, p = 0.004, **Table 1**).

Table 1: Correlation results of QASA, BI parameters, detrended TRW, mean temperature, precipitation, and $\delta^{13}C$.

Index (QASA)	Variable	Correlation (r)	p-value	Strength	Significance
Detrended TRW	Mean Temp (Erbil)	-0.20886	0.04113	Weak	Significant
	Mean Temp (Duhok)	-0.21664	0.034	Weak	Significant
	Precipitation (Erbil)	0.12613	0.22076	Weak	Not significant
	Precipitation (Duhok)	0.14323	0.16386	Weak	Not significant
EWBI	Mean Temp (Erbil)	-0.3782	1.45E-04	Moderate	Highly significant

	Mean Temp (Duhok)	-0.3806	1.31E-04	Moderate	Highly significant
	Precipitation (Erbil)	0.26994	0.00782	Weak	Very significant
	Precipitation (Duhok)	0.25048	0.01384	Weak	Significant
	δ13C	-0.22319	2.88E-02	Weak	Significant
LWBI	Mean Temp (Erbil)	0.01832	8.59E-01	Negligible	Not significant
	Mean Temp (Duhok)	0.02509	8.08E-01	Negligible	Not significant
	Precipitation (Erbil)	0.22803	0.02545	Weak	Significant
	Precipitation (Duhok)	0.16716	0.10357	Weak	Not significant
	δ13C	0.08249	0.42426	Negligible	Not significant
ΔBI	Mean Temp (Erbil)	0.36394	2.67E-04	Moderate	Highly significant
	Mean Temp (Duhok)	0.3727	1.84E-04	Moderate	Highly significant
	Precipitation (Erbil)	-0.0249	0.80973	Negligible	Not significant
	Precipitation (Duhok)	-0.06612	0.52214	Negligible	Not significant
	δ13C	0.28437	0.00499	Weak	Very significant

The series analysis shows that mean temperature increased steadily since approximately 1980, up to the present. The BI parameters reflect this warming trend: EWBI values have decreased since the early 1980s (**Fig. 7a**), detrended TRW is characterized by reduced values growth, and ΔBI values have increased (**Fig. 5c and d**). The variability of LWBI is relatively stable over the record, showing weak interannual variability (**Fig. 6a and b**).

https://doi.org/10.5194/egusphere-2026-4943
Preprint. Discussion started: 28 September 2026

The overall evidence shows that temperature is the dominant factor that controls the features of tree growth and wood density in the Kurdistan region. Although precipitation is a secondary positive factor on the development of earlywood, the effect of precipitation is insufficient to overcome suppressing effect of increasing temperatures on total ring width. The opposite behavior of EWBI (negative with temperature, positive with precipitation) and ΔBI (positive with temperature, positive with $\delta^{13}C$) (**Table 1, Fig. 6 and Fig. 7**) provides complementary information regarding the dynamics of seasonal wood formation. All these proxies taken together show that the shift to reduced earlywood production, increased latewood-earlywood contrast and lower total growth of trees in the study area since the beginning of sustained warming around 1980 have produced a distinct fingerprint of regional climate change in the anatomical and isotopic archives of the trees.

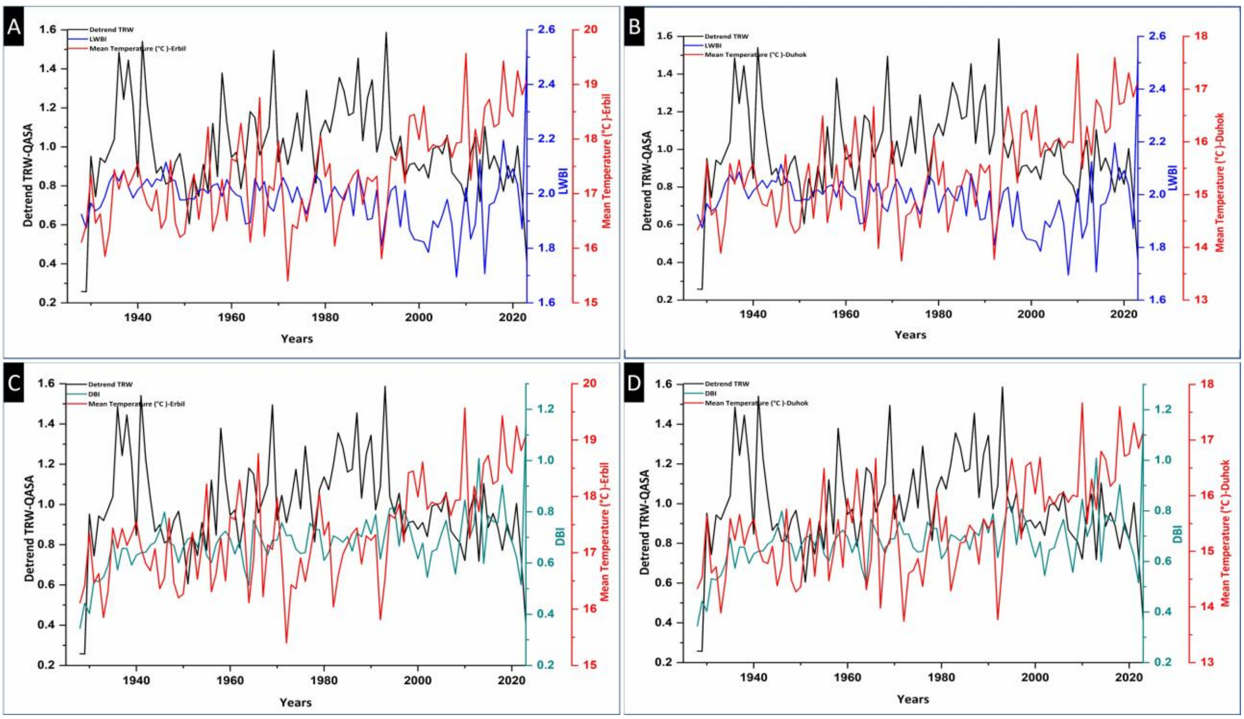

Figure 6: QASA time-series panels (a-d) showing detrended tree ring width (TRW) and blue-intensity (BI) parameters with temperature. Panels a and b: LWBI remains relatively stable through the record with no strong temperature sensitivity; detrended TRW shows a post-1980 decline consistent with warming-limited growth for both Erbil and Duhok. Panels c and d: ΔBI rises after 1980 and is positively and significantly linked to temperature, indicating increased latewood-earlywood contrast for Erbil and Duhok.

https://doi.org/10.5194/egusphere-2026-4943
Preprint. Discussion started: 28 September 2026

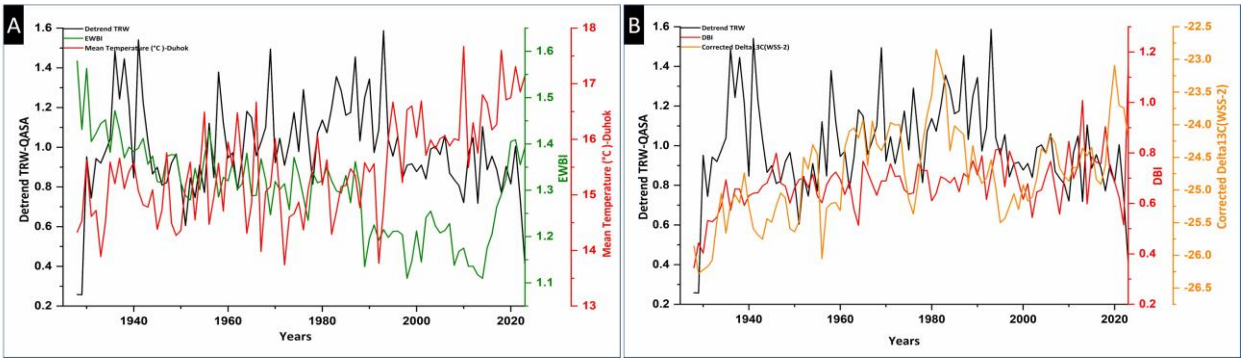

Figure 7: QASA time-series panels (a-b) showing detrended TRW and BI parameters with temperature and δ¹³C. Panel a TRW declines after 1980, EWBI is negatively correlated with temperature, with a pronounced decline since 1980, indicating reduced earlywood production in warmer years. Panel b ΔBI is positively associated with δ¹³C, highlighting physiological responses (increased water-use efficiency) that accompany enhanced latewood contrast under warming.

3.1.2 *Juglans Regia* (WSS2)

The statistical findings of correlation for WSS2 reveal varied and relatively opposite climate predictors among the different parameters (**Table 2, Fig. 8 and Fig. 9**). Detrended TRW is weakly negatively correlated to mean temperature at Erbil ($r = -0.170$, $p = 0.089$) and Duhok ($r = -0.181$, $p = 0.070$) with marginal significance (**Table 2**). There are weak non-significant correlations with precipitation. The BI parameters indicate more significant signals. The EWBI and mean temperature are moderately and negatively correlated ($r = -0.366$ in Erbil and $r = -0.376$ in Duhok, both $p < -0.001$). The EWBI also shows a highly significant and negative relationship with δ¹³C ($r = -0.393$, $p < -0.001$) (**Table 2**). The correlations with the precipitation are positive with a low level of significance. LWBI with WSS2 has the strongest climate signal of all the measured parameters. It is highly significant and has a negative correlation, which is moderate with the mean temperature ($r = -0.444$ in Erbil, $r= -0.451$ in Duhok, $p < 0.001$) (**Table 2**), leading to the conclusion that the decreasing density or darkening of latewood is limited by warmer years. δ¹³C indicates no relationships. Precipitation correlations are also weak and non-significant. The ΔBI has a less substantial yet significant negative correlation with temperature ($r = -0.224$ in Erbil, -0.228 in Duhok, $p < 0.05$). This is an indication that warmer years decrease the latewood-earlywood contrast in WSS2, which is probably due to the suppression of both earlywood and latewood by heat stress. Interestingly, ΔBI also has a positive and very significant relationship with δ¹³C ($r = 0.295$, $p = 0.003$) demonstrating that the years that have greater water-use efficiency (because they have more positive δ¹³C values) tend to have higher values of ΔBI.

Table 2: Correlation results of WSS2, BI parameters, detrended TRW, mean temperature, precipitation, and δ¹³C.

Index (WSS2)	Variable	Correlation (r)	p-value	Strength	Significance
Detrended TRW	Mean Temp (Erbil)	-0.17062	0.08965	Weak	Marginal

https://doi.org/10.5194/egusphere-2026-4943
Preprint. Discussion started: 28 September 2026

	Mean Temp (Duhok)	-0.18137	0.07093	Weak	Marginal
	Precipitation (Erbil)	0.14288	0.15614	Weak	Not significant
	Precipitation (Duhok)	0.09765	0.3338	Negligible	Not significant
EWBI	Mean Temp (Erbil)	-0.36613	1.80E-04	Moderate	Highly significant
	Mean Temp (Duhok)	-0.37613	1.15E-04	Moderate	Highly significant
	Precipitation (Erbil)	0.18996	0.05836	Weak	Marginal
	Precipitation (Duhok)	0.16563	0.09958	Weak	Marginal
	δ13C	-0.39306	6.82E-05	Moderate	Highly significant
LWBI	Mean Temp (Erbil)	-0.44434	3.64E-06	Moderate	Highly significant
	Mean Temp (Duhok)	-0.45135	2.44E-06	Moderate	Highly significant
	Precipitation (Erbil)	0.1525	0.12985	Weak	Not significant
	Precipitation (Duhok)	0.15306	0.12843	Weak	Not significant
	δ13C	-0.0052	0.95968	Negligible	Not significant
ΔBI	Mean Temp (Erbil)	-0.22473	2.46E-02	Weak	Significant
	Mean Temp (Duhok)	-0.22889	0.02198	Weak	Significant
	Precipitation (Erbil)	0.05613	0.57912	Negligible	Not significant
	Precipitation (Duhok)	0.06838	0.49906	Negligible	Not significant

https://doi.org/10.5194/egusphere-2026-4943
Preprint. Discussion started: 28 September 2026

δ13C	0.29533	0.00332	Weak	Very significant

The increase in temperature that started in the early 1980s is demonstrated in the record of temperature and reflected in the BI parameters. Since 1980, EWBI has been declining steadily (**Fig. 9a**), LWBI has also decreased as well, and ΔBI trends downward. Detrended TRW shows a decrease in growth values within the same period (**Fig. 8a-d**), whereas $\delta^{13}C$ moves upwards (**Fig. 9b**). Such synchronous responses indicate that WSS2 trees are highly influenced by warming, and especially in the aspect of wood density characteristics.

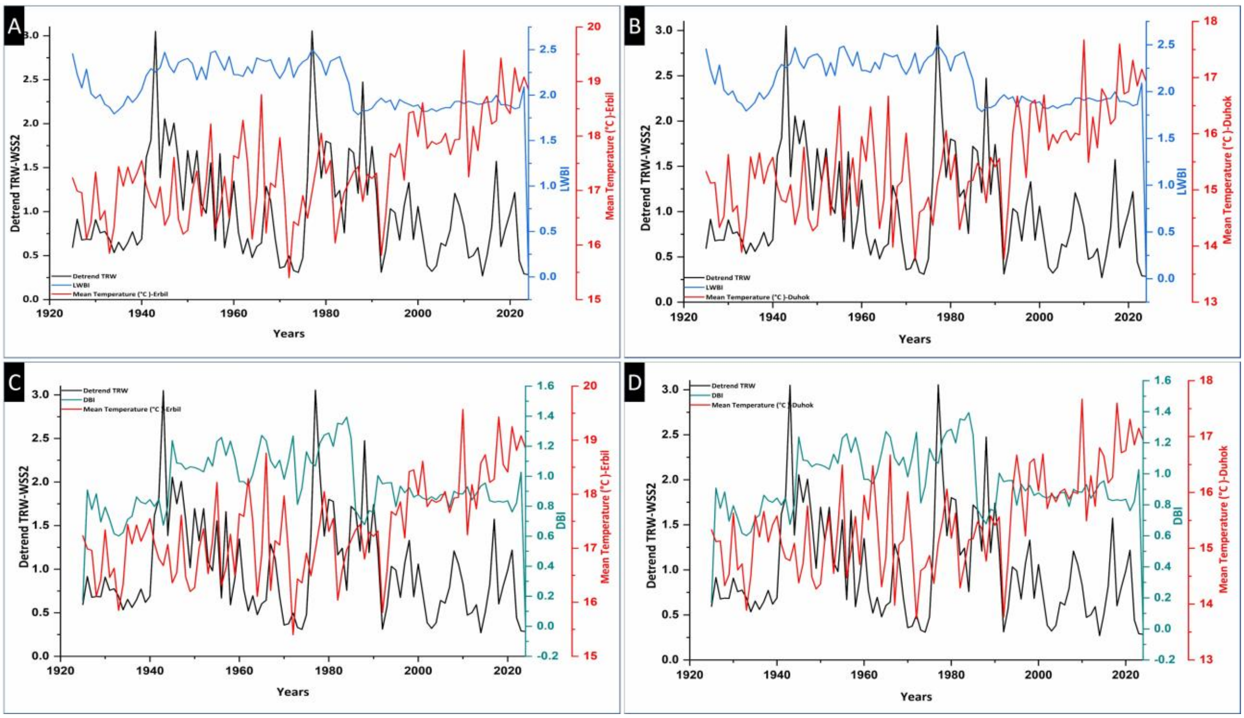

Figure 8: WSS2 time-series panels (a-d) showing detrended tree ring width (TRW) and blue-intensity (BI) parameters together with temperature and isotopic context. Panels a and b TRW declines after 1980, reflecting growth limitation under rising temperature; LWBI also decreases markedly after 1980 and is negatively correlated with temperature, confirming latewood sensitivity in both Erbil and Duhok. Panels c and d ΔBI shows a similar post-1980 decline in both sites, reflecting reduced earlywood-latewood contrast under warming.

https://doi.org/10.5194/egusphere-2026-4943
Preprint. Discussion started: 28 September 2026

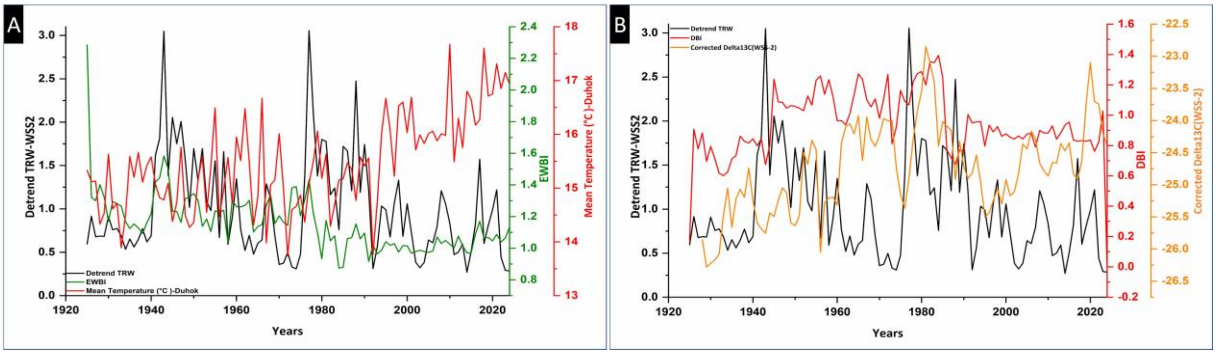

Figure 9: WSS2 time-series panels (a-b) showing detrended TRW and BI parameters with temperature and δ¹³C. Panel a TRW declines after 1980, while EWBI shows a clear downward trend and significant negative correlation with temperature, highlighting reduced earlywood development under warming. Panel b ΔBI also trends downward after 1980, but its positive relationship with δ¹³C indicates a physiological adjustment toward greater water-use efficiency under heat stress.

3.1.3 *Fraxinus* (Bnaw)

The correlation analysis of the Bnaw sample reveals that the overall climate sensitivity is relatively weak when compared to the samples of the other species (**Table 3, Fig. 10 and Fig. 11**). There are weak and non-significant positive correlations of detrended TRW with mean annual temperature ($r = 0.128$ in Erbil, $r = 0.122$ in Duhok) and precipitation ($r = 0.181$ in Erbil, $r = 0.076$ in Duhok) (**Table 3**). Such findings indicate that a radial growth in Fraxinus (Bnaw) trees is not strongly limited by the temperature or precipitation.

The BI parameters emphasize more specific climate responses. There is moderate and significant negative correlation of EWBI with mean temperature ($r = -0.347$ in Erbil, $r = -0.340$ in Duhok; both $p < 0.01$) (**Table 3**), meaning that warmer climate results in lower values of earlywood BI. The positive correlation with precipitation ($r = 0.194$ in Erbil, $r = 0.236$ in Duhok) are weak near significant or significant, indicating that warmer climates favor the increase of EWBI values. Notably, EWBI is negatively and significantly correlated with δ¹³C ($r = -0.293$, $p = 0.006$) (**Table 3**), indicating that years of increased earlywood intensity are associated with a lower δ¹³C. LWBI has a less strong, yet still very prominent climate signal. It has a negative and very significant correlation with mean temperature ($r = -0.279$ in Erbil and $r = -0.282$ in Duhok both $p < 0.01$), which indicates that higher temperatures suppress latewood intensity suggesting that the effect of temperature is a limiting factor because of its impact on the water availability, and precipitations have weak and only marginally significant relationship in Duhok ($r = 0.210$, $p = 0.052$) (**Table 3**). It shows a weakly negative and marginal correlation with δ¹³C ($r = -0.208$, $p = 0.056$), once again indicating that water-use efficiency is lower in years of higher latewood BI. Conversely, ΔBI is barely correlated with all the variables tested, including temperature, precipitation and δ¹³C (**Table 3**). This insignificance in signal suggests that in Bnaw, both the earlywood and latewood BI are not highly climate sensitive, possibly due to the similar response of both earlywood and latewood to interannual variability. This is contrary to QASA, in which ΔBI was positively correlated with temperature and WSS2, in which ΔBI was negatively correlated with temperature. In the case of *Fraxinus* (Bnaw), when there is no ΔBI signal, it could

https://doi.org/10.5194/egusphere-2026-4943
Preprint. Discussion started: 28 September 2026

indicate that species-characteristic anatomic mechanisms are responsible in determining how density contrast is expressed.

285 **Table 3: Correlation results of *Fraxinus* (Bnaw), BI parameters, detrended TRW, mean temperature, precipitation, and $\delta^{13}C$.**

Index (Bnaw)	Variable	Correlation (r)	p-value	Strength	Significance
Detrended TRW	Mean Temp (Erbil)	0.12853	0.24109	Weak	Not significant
	Mean Temp (Duhok)	0.12281	0.26284	Weak	Not significant
	Precipitation (Erbil)	0.18183	0.09582	Weak	Marginal
	Precipitation (Duhok)	0.07632	0.48757	Negligible	Not significant
EWBI	Mean Temp (Erbil)	-0.34746	0.00112	Moderate	Highly significant
	Mean Temp (Duhok)	-0.34094	0.00141	Moderate	Highly significant
	Precipitation (Erbil)	0.19449	7.45E-02	Weak	Marginal
	Precipitation (Duhok)	0.2365	0.02932	Weak	significant
	δ13C	-0.29372	0.00637	Weak	Very significant
LWBI	Mean Temp (Erbil)	-0.27998	0.00945	Weak	Very significant
	Mean Temp (Duhok)	-0.28288	0.00871	Weak	Very significant
	Precipitation (Erbil)	0.16807	0.12417	Weak	Not significant
	Precipitation (Duhok)	0.21068	0.05294	Weak	Marginal
	δ13C	-0.20802	0.05608	Weak	Marginal
ΔBI	Mean Temp (Erbil)	-0.08275	0.45148	Negligible	Not significant

https://doi.org/10.5194/egusphere-2026-4943
Preprint. Discussion started: 28 September 2026

Mean Temp (Duhok)	-0.09723	0.37602	Negligible	Not significant
Precipitation (Erbil)	0.06884	5.31E-01	Negligible	Not significant
Precipitation (Duhok)	0.09585	0.38285	Negligible	Not significant
δ13C	-0.01379	0.90032	Negligible	Not significant

The long-term trend since the early 1980s is observed most distinctly in the EWBI and LWBI chronologies as they start to decrease after 1980 coinciding with prolonged warming onset (**Fig. 10a-b and Fig. 11**). Though detrended TRW shows a slightly increasing tendency over that time. The corresponding reduction in EWBI and LWBI suggests that *Fraxinus* (Bnaw) is subjected to lower wood development during early and late seasons of growth in warmer environments, which supports the sensitivity of its BI parameters to recent climatic change.

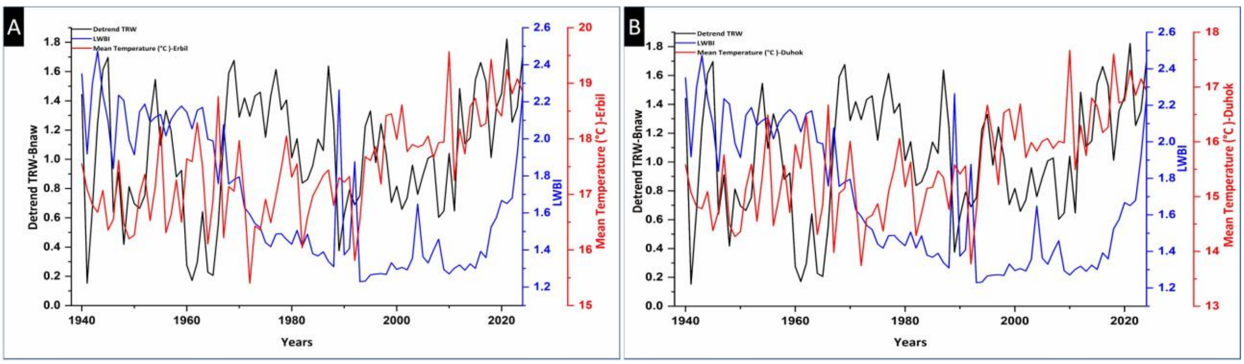

Figure 10: *Fraxinus* (Bnaw) time-series panels (a-b) showing LWBI with temperature and detrended TRW for Erbil and Duhok. LWBI declines after 1980, significantly negatively correlated with temperature, this reflects reduced latewood development under sustained warming, while Detrended TRW shows upward trend of growth.

https://doi.org/10.5194/egusphere-2026-4943
Preprint. Discussion started: 28 September 2026

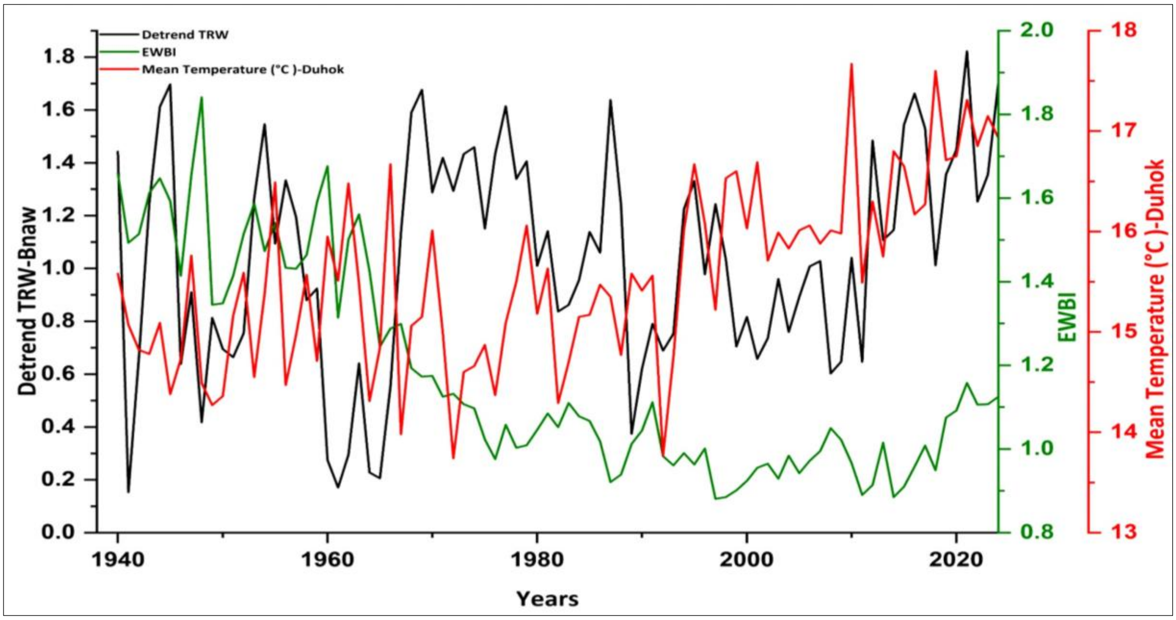

Figure 11: ***Fraxinus*** **(Bnaw) time-series of detrended TRW and EWBI verses temperature. Detrended TRW increasing since about 1980, EWBI negative correlations with temperature and decreasing since about 1980. Reflecting reduced wood formation during warmer years.**

3.2 Wavelet Coherence Analysis (R^2)

3.2.1 Climate-BI Coherence (Application to WSS2 Datasets)

1) EWBI vs Mean Temperature (a) Coherence is concentrated in the decadal band (≈8-12 yr) with intermittent multidecadal patches (≈15-30 yr). Notable, mostly significant lobes occur in the late-1930s-1940s, mid-1960s-1970s, late-1970s–mid-1980s, and late-1990s-2010s. Phase arrows in the late-1930s lobe are predominantly in-phase (→) indicating EWBI-temperature co-behavior at decadal scales (higher EWBI during warmer springs). Post-1980 decadal coherence is again mostly in-phase, implying a growing spring thermal control on earlywood optical properties. Overall, earlywood shifts from being primarily moisture-paced mid-century to mixed but increasingly temperature-paced since ~1980, consistent with regional warming and rising spring evaporative demand and long summers (**Fig. 12**).

https://doi.org/10.5194/egusphere-2026-4943
Preprint. Discussion started: 28 September 2026

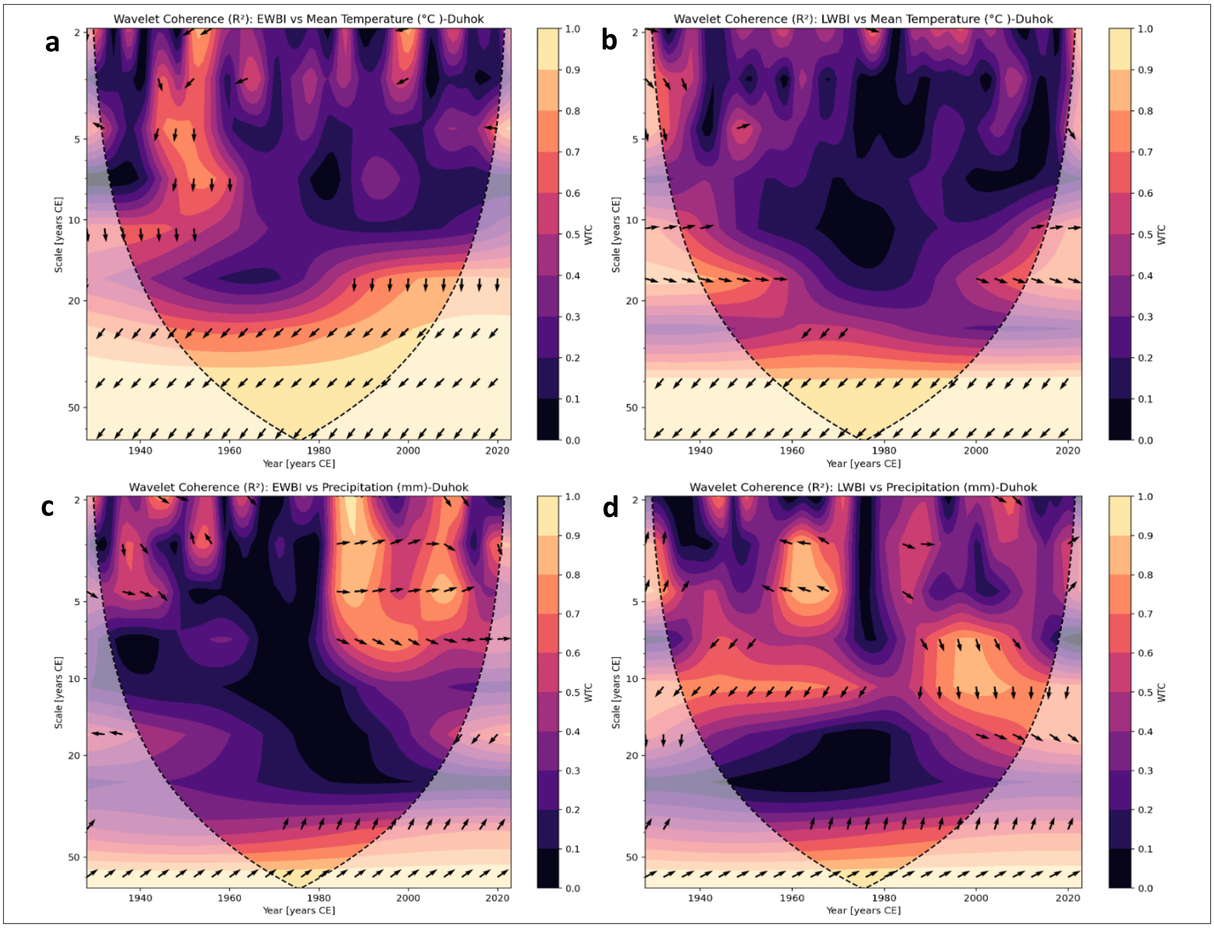

Figure 12: Continuous wavelet coherence (R2) maps (1925-2024) for tree-ring blue intensity and climate in Dohuk. (a) Earlywood blue intensity (EWBI) vs. temperature; (b) Latewood blue intensity (LWBI) vs. temperature; (c) EWBI vs. precipitation; (d) LWBI vs. precipitation. Color shows coherence strength; white contours mark significance; the dashed line is the cone of influence (COI). Arrows denote phase (→ in-phase, ← anti-phase, tilt = lag). Coherence and phase patterns reveal a shift from precipitation- to temperature-driven growth control, especially post-1980.

2) LWBI vs Mean Temperature (b)

Represents he strongest and most persistent relationship. Strong decadal (8--12 yr) and multi-decadal (15--30 yr) coherence spans the late-1930s--1950s, late-1970s-1990s, and 2000s-2010s; mostly inside the COI and frequently significant. Arrows are predominantly in-phase indicating higher LWBI coherence with warmer summers at these scales; slight forward-tilt suggests temperature tends to lead LWBI modestly. Hence, the latewood in Dohuk is thermally dominated, especially since 1980, reflecting warming and lengthening of the hot season (**Fig. 12**).

https://doi.org/10.5194/egusphere-2026-4943
Preprint. Discussion started: 28 September 2026

3) EWBI vs Precipitation (c)

Coherence is intermittent and generally weaker than LWBI-Temperature, with short inter-annual highs (2-5 yr) in drought windows and patchy decadal structure. Rare multi-year features appear during extended soil-moisture deficits. Significant patches often show anti-phase (←) indicating higher LWBI during lower precipitation, a heat/moisture-stress signature. In-phase pockets, when present, coincide with rare anomalous wet summers. In a nutshell, latewood responds more to temperature than to precipitation totals, consistent with hot, dry summers where evaporative demand governs late-season growth. Moisture events imprint at short periods but lack stable long-period pacing (**Fig. 12**).

4) LWBI vs Precipitation (d)

A clear multi-decadal lobe (15-30 yr) spans the 1930s-1950s, with decadal coherence into the 1960s-early 1970s (significant, inside COI). Post-1980, long-period organization weakens, while inter-annual/decadal bursts recur during dry springs. The mid-century arrows in figure tend to be in-phase →, implying higher EWBI with higher wetter winters/springs. Later decades show more mixed or anti-phase ← episodes, or mixed short periods arrows, reflecting variable spring moisture and greater temperature influence. Earlywood historically tracked precipitation-driven at long periods; in recent decades this pacing erodes, replaced by shorter, less organized episodes and an emerging temperature control (compare to Panel a) (**Fig. 12**).

The overall synthesis of the Climatic Shifts and Change Signals show that late-1930s warm episode (decadal) is concurrent significant lobes in EWBI-T and LWBI-T with arrows support a warm late-1930s; EWBI-P phase helps characterize accompanying moisture anomalies. The 1960s-mid-1970s transition is transitional where EWBI-P long-period coherence weakens while EWBI-T and LWBI-T decadal bands strengthen, a direct effect of transition from moisture to temperature control. The post-1980 thermal regime is strong, persistent at decadal/multi-decadal coherence in LWBI-T and recurrent decadal lobes in EWBI-T indicate tight temperature driving factor. The major event-scale shifts are within late-1990s-2000s where inter-annual islands across panels align with drought/heat highs, confirming proxy sensitivity to short-scale hydroclimate anomalies. In summary, the Dohuk wood-anatomy proxies reveal a climate-change fingerprint: a shift from precipitation-paced earlywood to temperature-dominated early- and latewood, especially after 1980, with interannual drought/heat events superimposed. This pattern is consistent with regional warming, higher evaporative demand, and increased hydroclimate variability.

3.2.2 BI, Detrended TRW vs. $\delta^{13}C$ Coherence

Here, the analysis of Squared Wavelet Coherence (WTC R2 Coherence) between year-to-year changes in wood blue intensity (ΔBI) and cellulose $\delta^{13}C$ from the Dohuk resolves how physiology and wood properties co-vary across time scales. The dominant coupling appears as a broad decadal band (~10-25 yr) that is largely inside the cone from the late 1930s through the 1970s, with weaker recurrence in parts of the 1990s-2000s. Shorter inter-annual (2-7 yr) islands punctuate the record most clearly around 1950-1962 and again in the late 1990s-2000s signalling event-scale droughts superimposed on slower variability

https://doi.org/10.5194/egusphere-2026-4943
Preprint. Discussion started: 28 September 2026

(**Fig. 13**). Across both the decadal lobe and the inter-annual islands, phase arrows are predominantly anti-phase (←), showing that Δδ¹³C increases when ΔBI decreases and vice versa. This sign matches the expected drought mechanism: reduced stomatal conductance under higher vapor-pressure deficit lowers isotopic discrimination (raising δ¹³C), while concurrent water limitation constrains cambial activity and cell-wall deposition, reducing BI. Arrow tilts within the decadal band indicate that Δδ¹³C often leads or coincides with ΔBI, consistent with rapid physiological adjustment followed by an integrated wood-property response over the growing season.

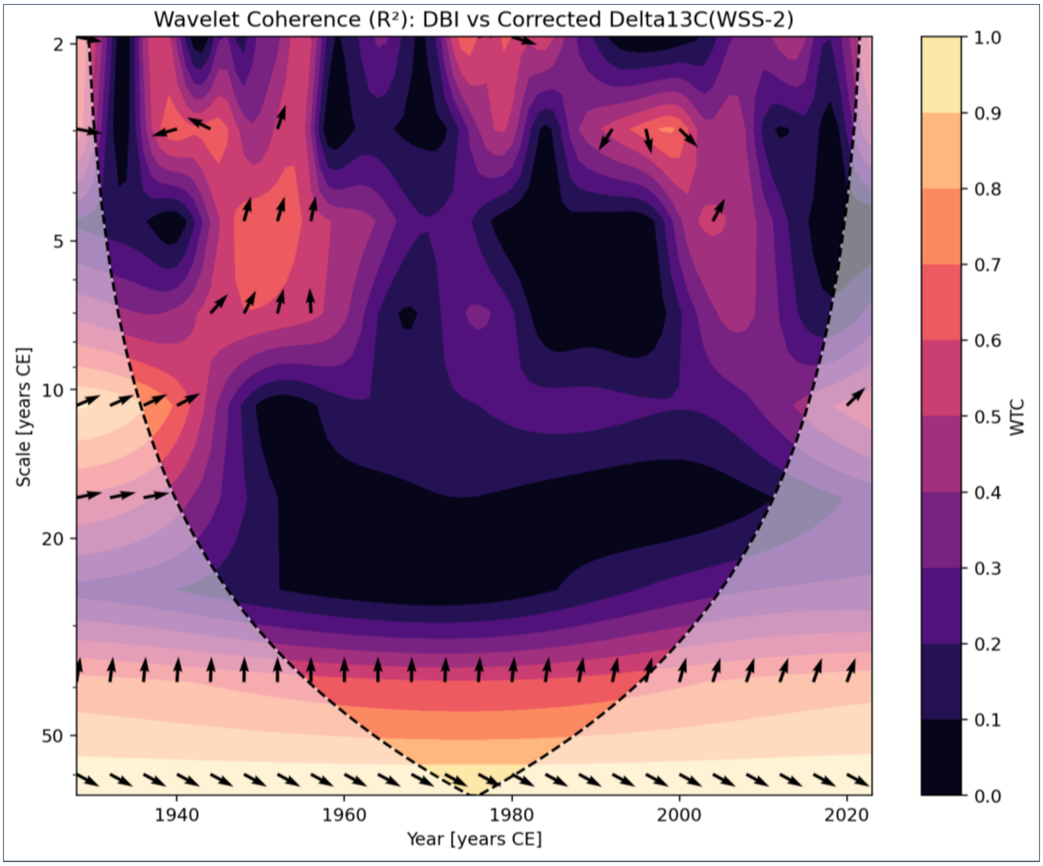

Figure 13: Squared wavelet coherence (WTC, R2) between year-to-year changes in blue intensity (ΔBI) and corrected tree ring δ¹³C (WSS-2) at Dohuk. Time is on the x-axis; period (years, log) on the y-axis; colors show coherence, the dashed curve is the cone of influence, and arrows indicate phase (→ in-phase, ← anti-phase; tilt = lead/lag). A broad decadal band (~10-25 yr) shows predominantly anti-phase coupling from the late-1930s to the 1970s, with interannual (2-7 yr) bursts marking drought events. A mid-1960s–mid-1980s low-coherence gap indicates non-stationary decoupling of ΔBI and δ¹³C, after which only short anti-phase patches recur.

The wavelet coherence map reveals a notable dark zone spanning the mid-1960s to mid-1980s at decadal scales (10-25 yr), where coherence drops to near zero. This low-coherence band is within the statistically reliable region (cone of influence), confirming it represents a real phenomenon rather than a plotting boundary effect. The breakdown indicates that wood density and isotopic discrimination, previously coupled through shared hydroclimate forcing, temporarily decoupled during this period

https://doi.org/10.5194/egusphere-2026-4943
Preprint. Discussion started: 28 September 2026

likely reflecting a shift in the dominant environmental controls on each proxy. Mechanistically, it is consistent with a regime shift in limiting factors (e.g., increasing temperature control on BI while $\delta^{13}C$ reflects mixed controls), physiological decoupling under sustained stress or changing CO_2 background (stomatal regulation diverging from carbon allocation), and/or a seasonal-window mismatch as climate timing changes. This low-coherence interval can be corroborated with scale-averaged coherence in the 8-12 and 15-25 yr bands, moving correlations with matched seasonal windows, and partial coherence controlling for temperature and precipitation. Climatically, the late 1930s-1940s present a coherent, anti-phase decadal episode consistent with a warm/dry shift; the 1950s-early 1960s show repeated 2-5-year anti-phase bursts typical of multi-year drought sequences; through the mid-1960s-1970s the decadal coupling persists but fragments, indicating the onset of non-stationarity; and from the mid-1980s to early 2000s coherence weakens broadly, with only short anti-phase inter-annual patches re-emerging after ~2005 (**Fig. 13**). Overall, the ΔBI-$\Delta\delta^{13}C$ coherence records a transition from sustained, decadal moisture regimes in the mid-20th century to episodic, event-scale stress in recent decades, consistent with regional warming, heightened evaporative demand, and increasing hydroclimate variability across the eastern Mediterranean. The wavelet coherence map reveals a notable dark zone spanning the mid-1960s to mid-1980s at decadal scales (10-25 yr), where coherence drops to near zero. This low-coherence band sits well within the statistically reliable region (cone of influence), confirming it represents a real phenomenon rather than a plotting boundary effect (**Fig. 13**). The breakdown indicates that wood density and isotopic discrimination, previously coupled through shared hydroclimate forcing, temporarily decoupled during this period, which likely reflects a shift in the dominant environmental controls on each proxy.

Figure 14 display wavelet coherence (WTC R2) between detrended TRW and $\delta^{13}C$ (Dohuk, 1925-2024). Inside the cone of influence, the dominant coupling occurs in a decadal band (~10-25 yr) from the late 1930s through the 1970s, with short inter-annual (2-7 yr) islands. Phase arrows in these regions are predominantly anti-phase (←), consistent with expected physiology: during drier/warmer episodes $\delta^{13}C$ rises (reduced stomatal discrimination) while TRW declines, and the reverse during wetter periods. Arrow tilt in several decadal lobes suggests $\delta^{13}C$ tends to lead or coincide with TRW, indicating rapid physiological adjustment followed by an integrated growth response.

https://doi.org/10.5194/egusphere-2026-4943
Preprint. Discussion started: 28 September 2026

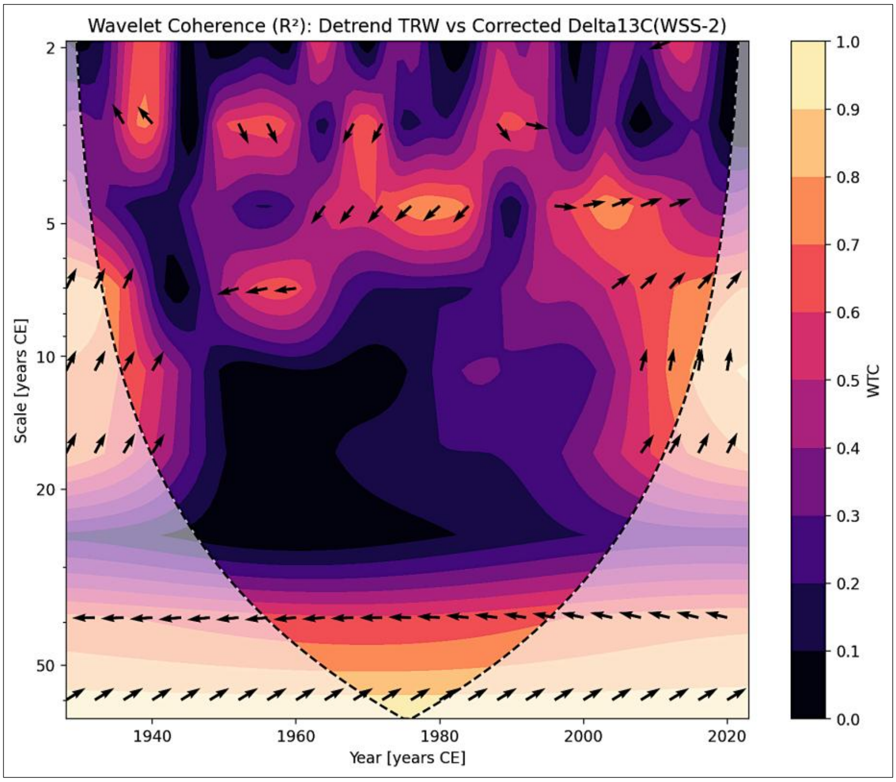

Figure 14: Continuous wavelet coherence (R2) map of detrended tree ring width (TRW) and corrected δ¹³C, Dohuk, 1925-2024. Strong decadal-scale coupling (10-25 yr) dominates from the late 1930s to mid-1970s, with anti-phase relationships indicating growth declines and isotopic stress during droughts. A distinct low-coherence zone at decadal scales in the late 1970s-early 1990s signals a breakdown in tree growth-physiology linkage, reflecting a period of non-stationary climate forcing. Post-2000, coherence recovers mainly at interannual scales, highlighting the growing influence of extreme events under intensified regional climate change.

A prominent low-coherence band spanning roughly the mid-1960s to mid-1980s (decadal scales) lies well inside the COI, indicating genuine non-stationarity in the TRW-δ¹³C relationship rather than an edge artifact. Possible contributors include a shift in limiting factors (greater temperature control), seasonal-window mismatch, stand dynamics, and rising CO_2 effects; these mechanisms are hypotheses that warrant testing (e.g., scale-averaged coherence, moving correlations, and partial coherence controlling for T, P). From ~2005 onward, coherence reappears mainly at inter-annual to short-decadal scales, whereas multi-decadal organization remains weak, implying that event-scale extremes increasingly synchronize the proxies, but sustained multi-year pacing has diminished (**Fig. 14**). Overall, the map records a transition from stable decadal moisture pacing in the mid-20th century to more episodic, thermally driven variability in recent decades consistent with regional warming and increased evaporative demand. Similarly, to **Figure 13** above, a prominent low-coherence band from the mid-1960s to mid-1980s at decadal periods (~10-25 yr) lies well within the COI, marking a true loss of coupling between TRW and δ¹³C (non-stationarity) rather than an edge effect where the two proxies no longer move together in a consistent phase i.e., the coupling between growth and isotope physiology is temporarily absent or highly variable. This interval likely reflects a regime shift in limiting processes and should be highlighted as a key climate-change fingerprint.

https://doi.org/10.5194/egusphere-2026-4943
Preprint. Discussion started: 28 September 2026

Wavelet coherence analysis of Dohuk total ring width (TRW) and mean temperature (1925-2024) reveals pronounced climate growth coupling (**Fig. 15**). From the late 1930s to mid-1970s, strong coherence at decadal (8-15 yr) and multi-decadal (25-40 yr) periods is marked by leftward (anti-phase) arrows, indicating suppressed growth during prolonged warm intervals a signature of drought or heat stress. Arrow direction and tilt indicate temperature anomalies typically precede ring narrowing, capturing the lead-lag dynamics of Mediterranean forest response.

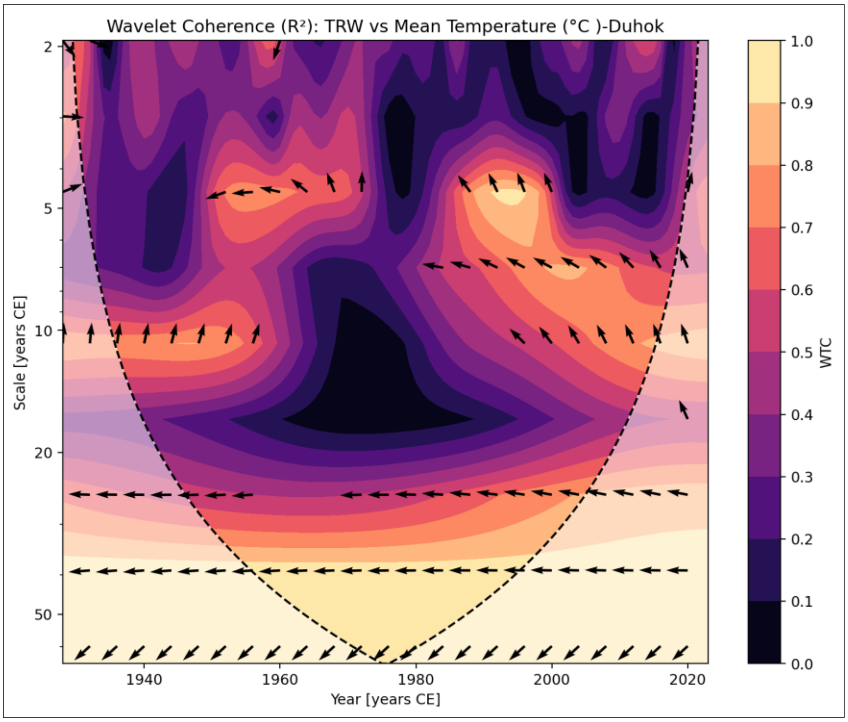

Figure 15: Continuous wavelet coherence (R^2) map between Duhok tree ring width (TRW) and mean temperature (1925-2024). Color shading represents the strength of coherence, and the dashed curve marks the cone of influence (COI) where edge effects become significant. Leftward and tilted arrows indicate anti-phase relations, with temperature anomalies leading reductions in growth. Strong decadal-to-multidecadal coherence (8-40 yr) dominates from the late 1930s to mid-1970s, weakens around the mid-1960s-1980s transition, and re-emerges after 1980 as a persistent temperature-controlled growth regime linked to regional warming.

A pronounced loss of coherence at decadal scales occurs from the mid-1960s to about 1980, forming a central dark wedge within the cone of influence that reflects a period of non-stationary climate growth linkage. This regime shift likely arises from increasing climate variability, rapid warming, altered precipitation patterns, and ecological stress, disrupting previously stable associations. Following 1980, the coherence structure transforms: decadal-band anti-phase coupling resurges, marking the emergence of a thermally dominated growth regime. Episodic, patchy in-phase relationships at shorter scales (2-5 years) are apparent in isolated early intervals but become rare as warming intensifies (**Fig. 15**). As a whole, the map shows a clear transition from varied and sometimes weak early temperature growth coupling, through a period of instability, into a modern regime characterized by persistent, temperature-driven suppression of tree growth at decadal and longer scales. These

https://doi.org/10.5194/egusphere-2026-4943
Preprint. Discussion started: 28 September 2026

coherence and phase patterns provide compelling evidence for shifting climate controls and highlight the ecological impact of regional warming and hydroclimate change in the eastern Mediterranean.

In contrast, the TRW precipitation map (**Fig. 16**) shows strongest, persistent in-phase coherence (rightward and down-right arrows) at inter-annual to short-decadal periods (~3-10 yr), most pronounced in the mid-20th century and after 1995. These zones indicate that precipitation reliably paces tree growth, with rainfall anomalies often leading TRW changes. Coherence at periods longer than ~20 years is weak or unstable, suggesting limited multi-decadal organization. A weakened mid-century band (~8-20 yr, 1955-mid-1980s) suggests non-stationary climate growth relations, echoing the temperature map's regime shift. The 40-50-year band observed in the TRW vs precipitation CWT R^2 map between roughly 1965 and 1995 shows a localized patch of moderate to strong coherence, well within the cone of influence. This zone is marked by predominantly rightward (in-phase) arrows, indicating that multi-decadal wet and dry cycles during this period were consistently mirrored in tree growth: extended wet (or dry) intervals led to broadly wider (or narrower) rings.

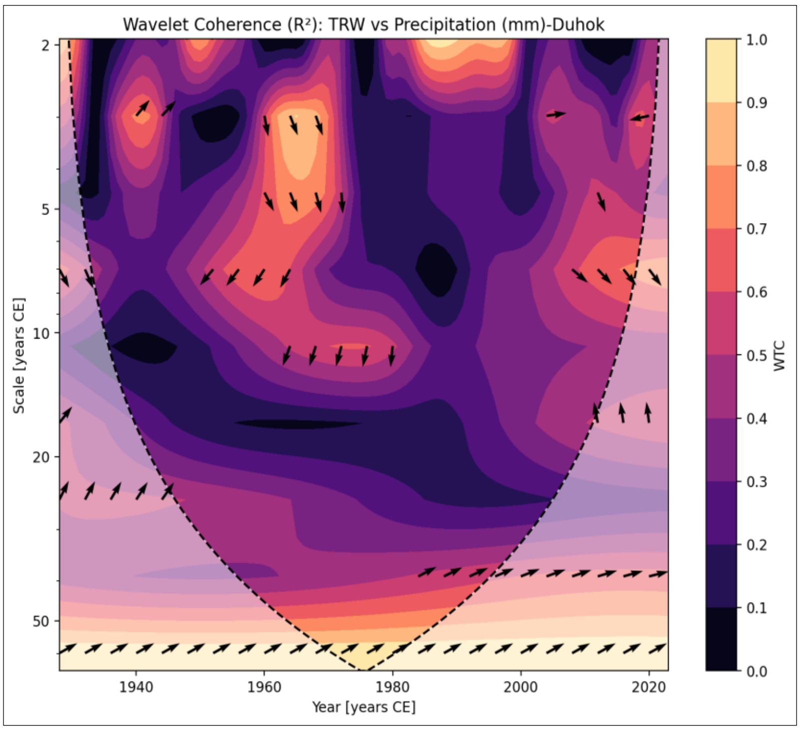

Figure 16: Continuous wavelet coherence (R^2) map between Duhok tree ring width (TRW) and precipitation (1925-2020). Coherence intensity increases from cool to warm colors; the dashed line outlines the cone of influence (COI). Rightward and down-right arrows mark in-phase relations where rainfall enhances tree growth. Persistent interannual-to-short-decadal coherence (~3-10 yr) appears during the mid-20th century and after 1995, while weakened coherence from 1955 to 1985 indicates non-stationary climate–growth coupling. A 40-50-year coherence band (1965-1995) reflects multi-decadal wet-dry cycles mirrored in ring-width variability.

Collectively, these patterns demonstrate a climatic transition: mid-20th-century tree growth in Dohuk was primarily moisture-driven at inter-annual scales, but since the 1980s, intensified warming has imposed persistent, decadal-scale temperature

https://doi.org/10.5194/egusphere-2026-4943
Preprint. Discussion started: 28 September 2026

limitation. Precipitation now exerts mainly episodic, event-scale control on growth. The direction and coherence of phase arrows precisely delineate both the historical drivers and the shifting sensitivities of Mediterranean trees under regional climate change.

4 Discussion

During the growing season, earlywood and latewood form at different times, and seasonal variations in climate exert an influence on their formation (Rossi et al., 2007, Begum et al., 2012). According to Oberhuber et al. (2011), earlywood is particularly affected by the early-season climate and relies to a larger degree on reserves of stored carbohydrates (Rahman et al., 2016) compared with earlywood formation. As stated by Lebourgeois (2000), latewood formation is more susceptible to the current year's climate than earlywood formation. The earlywood width increases during wet springs and warm summers, while extreme temperature excursions in Mediterranean sites can result in high latewood proportions (Camarero et al., 2021). The BI parameters give additional details about these seasonal processes. EWBI offers useful climatic data for the early growing season, despite being used in relatively few studies so far (Wilson et al., 2021, Cao et al., 2022). The main BI parameters that are employed to reconstruct summer temperature variation from conifer sites growing in temperature-limited environments, are LWBI and ΔBI (Björklund et al., 2015, Li and Li, 2023, Agapova et al., 2024).

In this study, the correlation analysis of BI parameters, climate variables (temperature and precipitation) and detrended TRW, coupled with $\delta^{13}C$, showed that there are noticeable climatic controls over the wood-formation dynamics in the northern part of Iraq. The complete series was taken as a single segment, and correlations were applied. Through chronology development, the initial heavy detrending of TRW eliminated small yet significant signals of climatic data, so a negative exponential detrending technique was utilized so that the finer signals could be preserved. In the BI measurements with CooRecorder, sometimes the first (pith) and last (bark) rings were abnormal. As is typical of other BI studies (Campbell et al., 2007, Björklund et al., 2014), these irregularities have been surmised to be caused by edge effects and optical artifacts in the scanning and image acquisition process. They were thus recorded but not used as climate indicators. The low mean inter-series correlation values of the LWBI data can be attributed to wood discoloration, the lack of resolution in the scanned images, or the existence of resin channels that affect light reflectance and collectively, diminish signal coherence and decrease correlations between trees (Rydval et al., 2014, Rydval et al., 2018).

The location of the site and its relationship to lower and upper tree-line are critical determining factor influencing the type of climate data stored in tree-rings and their measurements (Wilson and Hopfmueller, 2001, Sidor et al., 2015, Lyu et al., 2017). Studies on the Bavarian Forest and the Austrian Alps have shown that high altitude chronologies appear more effective in reconstructing past temperatures while low altitude chronologies are better in reconstructing past precipitation (Wilson et al., 2005, Leal et al., 2007). The WSS2 has a strong temperature signal but Bnaw and QASA have mixed or moisture-related responses. In the *Quercus Aegilops (QASA)* sample the detrended TRW is negatively correlated with mean temperature (**Table 1**), with no significant effect of precipitation. This type of negative TRW-temperature relationship is common in semi-arid and

https://doi.org/10.5194/egusphere-2026-4943
Preprint. Discussion started: 28 September 2026

Mediterranean-type locations where moisture shortage is intensified by high evaporation demand in warm climes (Campelo et al., 2013).

The EWBI exhibited negative and highly significant correlation with mean temperature positive correlation with precipitation (**Table 1**). Such associations also demonstrate that earlywood production increases during cooler and wetter years , with greater BI values, and inhibited in warmer conditions (García-González and Souto-Herrero, 2023). The negative correlation of EWBI with $\delta^{13}C$ is weak but significant. It is likely implies that increased EWBI value correlates with decreased $\delta^{13}C$, which means increased stomatal conductance and reduced intrinsic water-use efficiency in moist years (Farquhar et al., 1989, McCarroll and Loader, 2004). Earlywood sensitivity to spring moisture patterns is well-known in other regions, such as Mediterranean pines, where a strong relationship between earlywood formation and spring precipitation has been described (Campelo et al., 2007, Novak et al., 2013) and even in oak (González and Eckstein, 2003). The LWBI does not respond to temperature. Weaker annual temperature responses in latewood have also been reported in other BI based studies (Björklund et al., 2014). The ΔBI turns out to be a strong predictor of temperature variability, since higher evaporative demand by warm condition causes stomata to close, intrinsic water-use efficiency to increase, and latewood cell-wall thickening to be promoted compared to earlywood (Hong et al., 2023). The correlation with precipitation is negligible (**Table 1**). Together, the result of both decreasing EWBI and increasing ΔBI thus provide a coherent record of change in wood structure as a result of warming. According to recent studies ΔBI constitutes a more robust parameter for capturing high-frequency variability of temperature than traditional ring-width parameters (Zheng and Wilson, 2024, Song et al., 2025). Zheng and Wilson (2024) showed that ΔBI had a stronger relationship with temperature than LWBI in subtropical China. A multi-species study from the Great Basin of Nevada, USA found that LWBI shows high variation among species and elevation (King et al., 2025). However, there are exceptions; e.g., a Caucasus network showed stable and high LWBI temperature correlations at upper sites of the treeline (Dhyani et al., 2025), which outlines the context-dependent character of LWBI signals.

Figures 6 and 7 show independent proxies (detrended TRW and BI parameters with temperature and $\delta^{13}C$) synchronized. They suggest that the warming that has been experienced since 1980 has placed successively strong limits on radial growth, and on earlywood production, also it is causing an increase in the representation of latewood within annual rings. This is in line with the findings of Zhang et al. (2024), who demonstrated that dry years favor a greater *Latewood to Earlywood Ratio (LER)*, a proportional shift driven primarily by earlywood suppression rather than increased latewood production. These shifts indicate high sensitivity to drought and high drought resistance. This proportional change to latewood, along with slowed radial growth during dry years, could be an adaptive response to extreme drought (Zhang et al., 2024). A similar process could be involved in the oak response observed here. Other dendroclimatic studies of Middle East and Mediterranean Basin also report similar turning points with the 1980s indicating an important triggering point in the relationship between climate and growth in drought prone areas (Touchan et al., 2005, Linares et al., 2011, Dorado-Liñán et al., 2017). The overall evidence shows that temperature is the dominant factor that controls the features of tree growth and wood density in the region. In the case of *Juglans Regia* (WSS2), (**Table 2**) detrended TRW was negatively correlated to mean temperature with non-significant correlations of precipitation. These results suggest that a higher temperature tends to decrease the growth of rings. The EWBI

https://doi.org/10.5194/egusphere-2026-4943
Preprint. Discussion started: 28 September 2026

and mean temperature are negatively correlated, also with δ¹³C. This pattern suggests that WSS2 earlywood is more sensitive to cool and moist growing seasons, with higher values of EWBI representing favorable spring conditions. The years of higher EWBI are associated with lower values of δ¹³C, as it is correlated with increased stomatal conductance and decreased water use efficiency in the conditions of high moisture (McCarroll and Loader, 2004).

LWBI with WSS2 has the strongest climate signal of all the measured parameters. This means that BI of latewood in WSS2 represents a clear temperature-sensitive proxy, as during the colder the years, the latewood development appears stronger. Corresponding LWBI responses to temperature have been measured in conifers growing in northern Fennoscandian (Björklund et al., 2014). In addition, it is also reported by studies in temperate forests that latewood production is more susceptible to droughts in late spring to early summer than earlywood production, which supports the interpretation that latewood is the more climate sensitive component of tree growth (Martin-Benito et al., 2013). The ΔBI had significant negative correlation with temperature. ΔBI is designed to reduce the color bias of the BI data (Reid and Wilson, 2020). The reduced contrast of WSS2 might be a sign of the greater vulnerability of radial growth to warmer temperatures since a higher latewood-to-earlywood ratio has been associated with drought resistance in larch (Zhang et al., 2024). The ΔBI also had a positive relationship with δ¹³C These two signals indicate that ΔBI in WSS2 brings together wood-structural and physiological responses to climatic stress although it is less consistent when compared to EWBI and LWBI. The WSS2 shows a scenario in which both EWBI and LWBI decrease with warming (**Fig. 8 and Fig. 9**), resulting in a less stable ΔBI signal, as opposed to the commonly encountered scenario whereby the response of earlywood and latewood is the opposite. This type of species-specific anatomy strategy in the evolution of the dendroclimatic response aligns with the observations of studies of Mediterranean and semi-arid tree ring where diverse and sometimes contrasting wood-climate relationships are reported among species (Touchan et al., 2007, Arsalani et al., 2018).

The low climate sensitivity that observed in *Fraxinus* (**Fig. 10 and Fig. 11, Table 3**) is indeed in line with previous findings for ring-porous species, which are often attributed a muted growth-climate response. Roibu et al. (2020) observed higher climate sensitivity in earlywood than that latewood or total ring width in *Fraxinus excelsior*, implying reduced reliability of density-derived parameters for some species. Similarly, according to Bader et al. (2022), ring-porous species such as *Fraxinus* tend to have less drought sensitivity than diffuse-porous taxa. These results underscore the importance of multi-species analyses in producing strong paleoclimate reconstructions, because although all three species can capture the regional warming trend since the 1980s, the strength and expression of their BI-climate interactions differ significantly.

Altogether, the analysis indicates that EWBI is most robust and consistent in diagnosing the effects of climate across all the species and presents a strong negative response to increasing temperature and positive associations with precipitation and δ¹³C. The ΔBI proves to be the most consistent species-specific proxy within QASA, with significant positive relationships with both temperature and δ¹³C, and some valuable additional support in WSS2 and *Fraxinus* (Bnaw), but with more variable signal. Detrended TRW, however, only records weak climatic sensitivity when compared with BI.

The CWT R^2 Coherence Scalogram are used to show the relationship between two variables over time and at different time scales. It creates an $R^2(t,s)$ coherence scalogram map. Such a map indicates the strength of the relationship at each time and scale after smoothing (Torrence and Compo, 1998, Grinsted et al., 2004). The coherence maps highlight periods when the climate and tree data share common patterns, while phase arrows show whether one leads or lags the other or if they change together or oppositely (Grinsted et al., 2004). Interpretation focuses on the reliable center of the map called the *Cone of Influence* (COI) (**Figs. 12-16**) , with tests like AR (1) method to ensure the relationships are statistically meaningful and not coincidental (Torrence and Compo, 1998, Maraun et al., 2007). The results show that the BI method captures the impacts of recent warming in the region that offers an independent and complementary signal to standard ring-width and stable isotopes proxies. This study highlights the complexity of tree responses to climate by bringing together a number of BI parameters for various species, but also proves the possibility to enhance temperature reconstruction using BI-based techniques.

5 Conclusion

The integrated analysis of detrended TRW, BI parameters and $\delta^{13}C$ with temperature and precipitation shows multi-proxy evident of a significant shift in forest growth dynamics in the Kurdistan Region, which experienced climatic changes during the last decades. Increasing temperatures are the primary limiting factor for all species investigated, with the effect since the 1980s being stronger than the effect of precipitation. Changes in TRW, EWBI, and ΔBI signals under warming indicate reduced earlywood formation, altered latewood structure, and increased wood-density contrast. There is a significant coupling between structural and physiological response at the integration of BI parameters with $\delta^{13}C$, as higher intrinsic water-use efficiency (iWUE) under drought stress is correlated with reduced growth and density variability. However, Wavelet coherence analyses show a non-stationary coupling with temporal breakdowns and regime shifts in proxy relationships. Climate sensitivity varies among species, with *Quercus aegilops* and *Juglans regia* showing strong temperature responses, whereas *Fraxinus* displays a more moderate and complex behavior. These results show that Blue Intensity serves as a powerful and cost-effective alternative to conventional density measurements, effectively capturing long-term trends and high-frequency climate variability. This transition to temperature driven growth limitation indicates a heightened vulnerability of semi-arid forests to climate change, underscoring the necessity for multi-proxy approaches in climate reconstruction and ecosystem evaluation.

Supplement link

The link to the supplement will be included by Copernicus, if applicable.

Author contributions

Conceptualization: Kolo K. Methodology: Kolo K., Mohammed K.F., Clays P. Data curation: Kolo K., Mohammed K.F. Formal analysis: Kolo K., Mohammed K.F. Investigation: Mohammed K.F. Project administration: Kolo K., Mohammed K.F.,

https://doi.org/10.5194/egusphere-2026-4943
Preprint. Discussion started: 28 September 2026

Clays P. Supervision: Kolo K., Clays P. Validation: Kolo K., Mohammed K.F. Visualization: Kolo K., Mohammed K.F. Writing– original draft: Kolo K., Mohammed K.F., Clays P. Writing– review: Kolo K., Mohammed K.F., Clays P.

Competing interests

The authors declare that they have no conflict of interest.

Disclaimer

Copernicus Publications remains neutral with regard to jurisdictional claims made in the text, published maps, institutional affiliations, or any other geographical representation in this paper. While Copernicus Publications makes every effort to include appropriate place names, the final responsibility lies with the authors. Views expressed in the text are those of the authors and do not necessarily reflect the views of the publisher.

Acknowledgements

We thank the Faculty of Scientific Research and the Climate Change and Sustainability Research Center of Soran University for laboratory and technical support. Ph. Claeys acknowledges the support of the Research Foundation Flanders for Instrument purchase and the VUB Large Research Group and Strategic Program for laboratory maintenance and development. AI tools were strictly used for language support, such as English grammar verification.

Financial support

This study was financially supported by the OZR Basisfinanciering voor Grote Onderzoeksgroepen - AMGC

Review statement

The review statement will be added by Copernicus Publications listing the handling editor as well as all contributing referees according to their status anonymous or identified.

References

Agapova, V. V., Arzac, A., Kukarskih, V. V., Büntgen, U., Esper, J., and Kirdyanov, A. V.: Tree-ring blue intensity measurements from treeline sites in the Ural Mountains exhibit a strong summer temperature signal, Dendrochronologia, 88, 126267, https://doi.org/10.1016/j.dendro.2024.126267, 2024.

Arsalani, M., Bräuning, A., Pourtahmasi, K., Azizi, G., and Mohammadi, H.: Multiple tree-ring parameters of Quercus brantii Lindel in SW Iran show a strong potential for intra-annual climate reconstruction, Trees, 32, 1531–1546, https://doi.org/10.1007/s10086-003-0518-x, 2018.

Bader, M. K.-F., Scherrer, D., Zweifel, R., and Körner, C.: Less pronounced drought responses in ring-porous than in diffuse-porous temperate tree species, Agr. Forest Meteorol., 327, 109184, https://doi.org/10.1016/j.agrformet.2022.109184, 2022.

Barbosa, J. M. and Asner, G. P.: Effects of long-term rainfall decline on the structure and functioning of Hawaiian forests, Environ. Res. Lett., 12, 094002, https://doi.org/10.1088/1748-9326/aa7ee4, 2016.

Begum, S., Nakaba, S., Yamagishi, Y., Yamane, K., Islam, M. A., Oribe, Y., Ko, J.-H., Jin, H.-O., and Funada, R.: A rapid decrease in temperature induces latewood formation in artificially reactivated cambium of conifer stems, Ann. Bot., 110, 875–885, https://doi.org/10.1093/aob/mcs149, 2012.

Belmecheri, S. and Lavergne, A.: Compiled records of atmospheric CO2 concentrations and stable carbon isotopes to reconstruct climate and derive plant ecophysiological indices from tree rings, Dendrochronologia, 63, 125748,https://doi.org/10.1016/j.dendro.2020.125748, 2020.

Björklund, J., Gunnarson, B. E., Seftigen, K., Esper, J., and Linderholm, H.: Blue intensity and density from northern Fennoscandian tree rings, exploring the potential to improve summer temperature reconstructions with earlywood information, Clim. Past, 10, 877–885, https://doi.org/10.5194/cp-10-877-2014, 2014.

Björklund, J., Gunnarson, B. E., Seftigen, K., Zhang, P., and Linderholm, H. W.: Using adjusted blue intensity data to attain high-quality summer temperature information: a case study from Central Scandinavia, Holocene, 25, 547–556, https://doi.org/10.1177/0959683614562434, 2015.

Björklund, J., Fonti, M. V., Fonti, P., Van den Bulcke, J., and von Arx, G.: Cell wall dimensions reign supreme: cell wall composition is irrelevant for the temperature signal of latewood density/blue intensity in Scots pine, Dendrochronologia, 65, 125785, https://doi.org/10.1016/j.dendro.2020.125785, 2021.

Björklund, J., Seftigen, K., Kaczka, R. J., Rydval, M., and Wilson, R.: A definition and standardised terminology for Blue Intensity from Conifers, Dendrochronologia, 85, 126200, https://doi.org/10.1016/j.dendro.2024.126200, 2024.

Bradley, R. S.: Paleoclimatology: reconstructing climates of the Quaternary, Elsevier, 1999.

Breshears, D. D., Fontaine, J. B., Ruthrof, K. X., Field, J. P., Feng, X., Burger, J. R., Law, D. J., Kala, J., and Hardy, G. E. S. J.: Underappreciated plant vulnerabilities to heat waves, New Phytol., 231, 32–39, https://doi.org/10.1111/nph.17348, 2021.

https://doi.org/10.5194/egusphere-2026-4943
Preprint. Discussion started: 28 September 2026

Briffa, K. R., Osborn, T. J., Schweingruber, F. H., Jones, P. D., Shiyatov, S. G., and Vaganov, E. A.: Tree-ring width and density data around the Northern Hemisphere: Part 1, local and regional climate signals, Holocene, 12, 737–757, https://doi.org/10.1191/0959683602hl587rp, 2002.

Buckley, B. M., Hansen, K. G., Griffin, K. L., Schmiege, S., Oelkers, R., D'Arrigo, R. D., Stahle, D. K., Davi, N., Nguyen, T. Q. T., and Le, C. N.: Blue intensity from a tropical conifer's annual rings for climate reconstruction: an ecophysiological perspective, Dendrochronologia, 50, 10–22, https://doi.org/10.1016/j.dendro.2018.04.003, 2018.

Camarero, J. J., Collado, E., Martínez-De-Aragón, J., De-Miguel, S., Büntgen, U., Martinez-Peña, F., Martín-Pinto, P., Ohenoja, E., Romppanen, T., and Salo, K.: Associations between climate and earlywood and latewood width in boreal and Mediterranean Scots pine forests, Trees, 35, 155–169, https://doi.org/10.1007/s00468-020-02028-0, 2021.

Campbell, R., McCarroll, D., Loader, N. J., Grudd, H., Robertson, I., and Jalkanen, R.: Blue intensity in Pinus sylvestris tree-rings: developing a new palaeoclimate proxy, Holocene, 17, 821–828, https://doi.org/10.1177/0959683607080523, 2007.

Campbell, R., McCarroll, D., Robertson, I., Loader, N. J., Grudd, H., and Gunnarson, B.: Blue intensity in Pinus sylvestris tree rings: a manual for a new palaeoclimate proxy, Tree-Ring Res., 67, 127–134, https://doi.org/10.3959/2010-13.1, 2011.

Campelo, F., Nabais, C., Freitas, H., and Gutiérrez, E.: Climatic significance of tree-ring width and intra-annual density fluctuations in Pinus pinea from a dry Mediterranean area in Portugal, Ann. Forest Sci., 64, 229–238, https://doi.org/10.1051/forest:2006107, 2007.

Campelo, F., Vieira, J., and Nabais, C.: Tree-ring growth and intra-annual density fluctuations of Pinus pinaster responses to climate: does size matter? Trees, 27, 763–772, https://doi.org/10.1007/s00468-012-0831-3, 2013.

Cao, X., Hu, H., Kao, P.-K., Buckley, B. M., Dong, Z., Chen, X., Zhou, F., and Fang, K.: Improved spring temperature reconstruction using earlywood blue intensity in southeastern China, Int. J. Climatol., 42, 6204–6220, https://doi.org/10.1002/joc.7585, 2022.

Cernusak, L. A., Ubierna, N., Winter, K., Holtum, J. A., Marshall, J. D., and Farquhar, G. D.: Environmental and physiological determinants of carbon isotope discrimination in terrestrial plants, New Phytol., 200, 950–965, https://doi.org/10.1111/nph.12423, 2013.

Christiansen, B. and Ljungqvist, F. C.: Challenges and perspectives for large-scale temperature reconstructions of the past two millennia, Rev. Geophys., 55, 40–96, http://dx.doi.org/10.1002/2016RG000521, 2017.

Churakova, O. V., Fonti, M. V., Siegwolf, R. T., Saurer, M., and Myglan, V. S.: Impact of recent climate change on water-use efficiency strategies of Larix sibirica in the Altai-sayan mountain range, Forests, 11, 1103, https://doi.org/10.3390/f11101103, 2020.

Cook, E. R. and Peters, K.: The smoothing spline: a new approach to standardizing forest interior tree-ring width series for dendroclimatic studies, Tree-Ring Bulletin, 41, 45–53, 1981.

Cook, E. R., Krusic, P. J., Anchukaitis, K. J., Buckley, B. M., Nakatsuka, T., Sano, M., and Members, P. A. K.: Tree-ring reconstructed summer temperature anomalies for temperate East Asia since 800 CE, Clim. Dynam., 41, 2957–2972, https://doi.org/10.1007/s00382-012-1611-x, 2013.

D'Arrigo, R., Wilson, R., and Jacoby, G.: On the long-term context for late twentieth century warming, J. Geophys. Res.-Atmos., 111, https://doi.org/10.1029/2005JD006352, 2006.

Dhyani, R., Martin-Benito, D., Doğan, M., Kvaratskhelia, R., Köse, N., Güner, H. T., and Schneider, L.: Consistent summer temperature signals in a latewood blue intensity network from the upper tree line in the Caucasus, Dendrochronologia, 92, 126372, https://doi.org/10.1016/j.dendro.2025.126372, 2025.

Diefendorf, A. F., Mueller, K. E., Wing, S. L., Koch, P. L., and Freeman, K. H.: Global patterns in leaf 13C discrimination and implications for studies of past and future climate, P. Natl. Acad. Sci. USA, 107, 5738–5743, https://doi.org/10.1073/pnas.0910513107, 2010.

Dorado-Liñán, I., Zorita, E., Martínez-Sancho, E., Gea-Izquierdo, G., Di Filippo, A., Gutiérrez, E., Levanic, T., Piovesan, G., Vacchiano, G., and Zang, C.: Large-scale atmospheric circulation enhances the Mediterranean East-West tree growth contrast at rear-edge deciduous forests, Agr. Forest Meteorol., 239, 86–95, https://doi.org/10.1016/j.agrformet.2017.02.029, 2017.

Eschbach, W., Nogler, P., Schär, E., and Schweingruber, F. H.: Technical advances in the radiodensitometrical determination of wood density, Dendrochronologia, 13, 155–168, 1995.

Farquhar, G. D., Ehleringer, J. R., and Hubick, K. T.: Carbon isotope discrimination and photosynthesis, Annu. Rev. Plant Physiol. Plant Mol. Biol., 40, 503–537, https://doi.org/10.1146/annurev.pp.40.060189.002443, 1989.

Francey, R. and Farquhar, G.: An explanation of 13C/12C variations in tree rings, Nature, 297, 28–31, https://doi.org/10.1038/297028a0, 1982.

Fuentes, M., Salo, R., Björklund, J., Seftigen, K., Zhang, P., Gunnarson, B., Aravena, J.-C., and Linderholm, H. W.: A 970-year-long summer temperature reconstruction from Rogen, west-central Sweden, based on blue intensity from tree rings, Holocene, 28, 254–266, https://doi.org/10.1177/0959683617721322, 2018.

Fukazawa, K.: Ultraviolet microscopy, in: Methods in Lignin Chemistry, edited by: Lin, S. Y. and Dence, C. W., Springer, Berlin, Heidelberg, 110–121, https://doi.org/10.1007/978-3-642-74065-7_8, 1992.

García-González, I. and Souto-Herrero, M.: Earlywood anatomy highlights the prevalent role of winter conditions on radial growth of oak at its distribution boundary in nw iberia, Plants, 12, 1185, https://doi.org/10.3390/plants12051185, 2023.

George, S. S.: An overview of tree-ring width records across the Northern Hemisphere, Quaternary Sci. Rev., 95, 132–150, http://dx.doi.org/10.1016/j.quascirev.2014.04.029, 2014.

González, I. G. and Eckstein, D.: Climatic signal of earlywood vessels of oak on a maritime site, Tree Physiol., 23, 497–504, https://doi.org/10.1093/treephys/23.7.497, 2003.

Grinsted, A., Moore, J. C., and Jevrejeva, S.: Application of the cross wavelet transform and wavelet coherence to geophysical time series, Nonlin. Processes Geophys., 11, 561–566, https://doi.org/10.5194/npg-11-561-2004, 2004.

Hafner, P. and Levanič, T.: Stable carbon isotopes in Norway spruce (Picea abies (L.) Karst.) tree rings at two sites in Slovenia, Zbornik gozdarstva in lesarstva, 88, 43–52, 2009.

https://doi.org/10.5194/egusphere-2026-4943
Preprint. Discussion started: 28 September 2026

Harlow, B., Marshall, J., and Robinson, A.: A multi-species comparison of δ13C from whole wood, extractive-free wood and holocellulose, Tree Physiol., 26, 767–774, https://doi.org/10.1093/treephys/26.6.767, 2006.

Heeter, K. J., Harley, G. L., Maxwell, J. T., McGee, J. H., and Matheus, T. J.: Late summer temperature variability for the Southern Rocky Mountains (USA) since 1735 CE: applying blue light intensity to low-latitude Picea engelmannii Parry ex Engelm, Climatic Change, 162, 965–988, https://doi.org/10.1007/s10584-020-02772-9, 2020.

Heeter, K. J., Harley, G. L., Maxwell, J. T., Wilson, R. J., Abatzoglou, J. T., Rayback, S. A., Rochner, M. L., and Kitchens, K. A.: Summer temperature variability since 1730 CE across the low-to-mid latitudes of western North America from a tree ring blue intensity network, Quaternary Sci. Rev., 267, 107064, https://doi.org/10.1016/j.quascirev.2021.107064, 2021.

Hong, Y., Liu, X., Camarero, J. J., Xu, G., Zhang, L., Zeng, X., Aritsara, A. N. A., Zhang, Y., Wang, W., and Xing, X.: The effects of intrinsic water-use efficiency and climate on wood anatomy, Int. J. Biometeorol., 67, 1017–1030, https://doi.org/10.1007/s00484-023-02475-7, 2023.

Kaczka, R. J. and Wilson, R.: I-BIND: International Blue intensity network development working group, Dendrochronologia, 68, 125859, https://doi.org/10.1016/j.dendro.2021.125859, 2021.

Kaczka, R. J., Spyt, B., Janecka, K., Beil, I., Büntgen, U., Scharnweber, T., Nievergelt, D., and Wilmking, M.: Different maximum latewood density and blue intensity measurements techniques reveal similar results, Dendrochronologia, 49, 94–101, https://doi.org/10.1016/j.dendro.2018.03.005, 2018.

Keeling, R. F., Graven, H. D., Welp, L. R., Resplandy, L., Bi, J., Piper, S. C., Sun, Y., Bollenbacher, A., and Meijer, H. A.: Atmospheric evidence for a global secular increase in carbon isotopic discrimination of land photosynthesis, P. Natl. Acad. Sci. USA, 114, 10361–10366, https://doi.org/10.1073/pnas.1619240114, 2017.

Khider, D., Emile-Geay, J., Zhu, F., James, A., Landers, J., Ratnakar, V., and Gil, Y.: Pyleoclim: Paleoclimate Timeseries Analysis and Visualization with Python, Paleoceanogr. Paleocl., 37, e2022PA004509, https://doi.org/10.1029/2022PA004509, 2022.

Kienast, F., Schweingruber, F. H., Bräker, O. U., and Schär, E.: Tree-ring studies on conifers along ecological gradients and the potential of single-year analyses, Can. J. Forest Res., 17, 683–696, https://doi.org/10.1139/x87-111, 1987.

King, K. E., Cook, E. R., Krusic, P. J., and King, D. J.: Varying climate signals embedded in latewood blue intensity along an elevational gradient: A multi-species case study from the Great Basin, Nevada, USA, Dendrochronologia, 92, 126366, https://doi.org/10.1016/j.dendro.2025.126366, https://doi.org/10.1016/j.dendro.2025.126366, 2025.

Kohn, M. J.: Carbon isotope compositions of terrestrial C3 plants as indicators of (paleo) ecology and (paleo) climate, P. Natl. Acad. Sci. USA, 107, 19691–19695, https://doi.org/10.1073/pnas.1004933107, 2010.

Leal, S., Melvin, T. M., Grabner, M., Wimmer, R., and Briffa, K. R.: Tree-ring growth variability in the Austrian Alps: the influence of site, altitude, tree species and climate, Boreas, 36, 426–440, https://doi.org/10.1080/03009480701267063, 2007.

Lebourgeois, F.: Climatic signals in earlywood, latewood and total ring width of Corsican pine from western France, Ann. Forest Sci., 57, 155–164, https://doi.org/10.1051/forest:2000166, 2000.

Lee, H., Calvin, K., Dasgupta, D., Krinner, G., Mukherji, A., Thorne, P., Trisos, C., Romero, J., Aldunce, P., and Barret, K.: IPCC, 2023: Climate Change 2023: Synthesis Report, Summary for Policymakers, Contribution of Working Groups I, II and III to the Sixth Assessment Report of the Intergovernmental Panel on Climate Change, edited by: Lee, H. and Romero, J., IPCC, Geneva, Switzerland, https://doi.org/10.59327/IPCC/AR6-9789291691647.001, 2023.

Li, T. and Li, J.: August temperature reconstruction based on tree-ring latewood blue intensity in the southeastern Tibetan Plateau, Forests, 14, 1441, https://doi.org/10.3390/f14071441, 2023.

Linares, J. C., Tíscar, P. A., Camarero, J. J., Taïqui, L., Viñegla, B., Seco, J. I., Merino, J., and Carreira, J. A.: Tree growth decline on relict Western-Mediterranean mountain forests: Causes and impacts, Nova Science Publishers, Hauppauge, NY, USA, 2011.

Lyu, L., Suvanto, S., Nöjd, P., Henttonen, H. M., Mäkinen, H., and Zhang, Q.-B.: Tree growth and its climate signal along latitudinal and altitudinal gradients: comparison of tree rings between Finland and the Tibetan Plateau, Biogeosciences, 14, 3083–3095, https://doi.org/10.5194/bg-14-3083-2017, 2017.

Macdonald, F. A.: Deep-time paleoclimate proxies, AGU Adv., 1, e2020AV000244, https://doi.org/10.1029/2020av000244, 2020.

Mann, M. E., Zhang, Z., Hughes, M. K., Bradley, R. S., Miller, S. K., Rutherford, S., and Ni, F.: Proxy-based reconstructions of hemispheric and global surface temperature variations over the past two millennia, P. Natl. Acad. Sci. USA, 105, 13252–13257, https://doi.org/10.1029/1999gl900070_, 2008.

Maraun, D., Kurths, J., and Holschneider, M.: Nonstationary Gaussian processes in wavelet domain: Synthesis, estimation, and significance testing, Phys. Rev. E, 75, 016707, https://doi.org/10.1103/PhysRevE.75.016707, 2007.

Marchand, W., Girardin, M. P., Hartmann, H., Depardieu, C., Isabel, N., Gauthier, S., Boucher, É., and Bergeron, Y.: Strong overestimation of water-use efficiency responses to rising CO2 in tree-ring studies, Glob. Change Biol., 26, 4538–4558, https://doi.org/10.1111/gcb.15166, 2020.

Martin-Benito, D., Beeckman, H., and Canellas, I.: Influence of drought on tree rings and tracheid features of Pinus nigra and Pinus sylvestris in a mesic Mediterranean forest, Eur. J. Forest Res., 132, 33–45, https://doi.org/10.1007/s10342-012-0652-3, 2013.

Maxwell, R. S. and Larsson, L.-A.: Measuring tree-ring widths using the CooRecorder software application, Dendrochronologia, 67, 125841, https://doi.org/10.1016/j.dendro.2021.125841, 2021.

McCarroll, D. and Loader, N. J.: Stable isotopes in tree rings, Quaternary Sci. Rev., 23, 771–801, https://doi.org/10.1016/j.quascirev.2003.06.017, 2004.

McCarroll, D., Pettigrew, E., Luckman, A., Guibal, F., and Edouard, J.-L.: Blue reflectance provides a surrogate for latewood density of high-latitude pine tree rings, Arct. Antarct. Alp. Res., 34, 450–453, https://doi.org/10.1080/15230430.2002.12003516, 2002.

https://doi.org/10.5194/egusphere-2026-4943
Preprint. Discussion started: 28 September 2026

Novak, K., De Luis, M., Raventós, J., and Čufar, K.: Climatic signals in tree-ring widths and wood structure of Pinus halepensis in contrasted environmental conditions, Trees, 27, 927–936, https://doi.org/10.1007/s00468-013-0845-5, 2013.

Oberhuber, W., Swidrak, I., Pirkebner, D., and Gruber, A.: Temporal dynamics of nonstructural carbohydrates and xylem growth in Pinus sylvestris exposed to drought, Can. J. Forest Res., 41, 1590–1597, https://doi.org/10.1139/x11-084, 2011.

Pawelczyk, S., Pazdur, A., and Halas, S.: Stable carbon isotopic composition of tree rings from a pine tree from Augustów Wilderness, Poland, as a temperature and local environment conditions indicator, Isot. Environ. Healt. S., 40, 145–154, https://doi.org/10.1080/10256010410001671032, 2004.

Rahman, M. H., Begum, S., Nakaba, S., Yamagishi, Y., Kudo, K., Nabeshima, E., Nugroho, W. D., Oribe, Y., and Funada, R.: Relationship between the earlywood-to-latewood transition and changes in levels of stored starch around the cambium in locally heated stems of the evergreen conifer Chamaecyparis pisifera, Trees, 30, 1619–1631, https://doi.org/10.1007/s00468-016-1395-4, 2016.

Reid, E. and Wilson, R.: Delta blue intensity vs. maximum density: A case study using Pinus uncinata in the Pyrenees, Dendrochronologia, 61, 125706, https://doi.org/10.1016/j.dendro.2020.125706, 2020.

Roibu, C.-C., Sfeclă, V., Mursa, A., Ionita, M., Nagavciuc, V., Chiriloaei, F., Leşan, I., and Popa, I.: The climatic response of tree ring width components of ash (Fraxinus excelsior L.) and common oak (Quercus robur L.) from Eastern Europe, Forests, 11, 600, https://doi.org/10.3390/f11050600, 2020.

Rossi, S., Deslauriers, A., Anfodillo, T., and Carraro, V.: Evidence of threshold temperatures for xylogenesis in conifers at high altitudes, Oecologia, 152, 1–12, https://doi.org/10.1007/s00442-006-0625-7, 2007.

Rydval, M., Larsson, L.-Å., McGlynn, L., Gunnarson, B. E., Loader, N. J., Young, G. H., and Wilson, R.: Blue intensity for dendroclimatology: should we have the blues? Experiments from Scotland, Dendrochronologia, 32, 191–204, https://doi.org/10.1016/j.dendro.2014.04.003, 2014.

Rydval, M., Druckenbrod, D. L., Svoboda, M., Trotsiuk, V., Janda, P., Mikoláš, M., Čada, V., Bače, R., Teodosiu, M., and Wilson, R.: Influence of sampling and disturbance history on climatic sensitivity of temperature-limited conifers, Holocene, 28, 1574–1587, https://doi.org/10.1177/0959683618782605, 2018.

Saurer, M. and Siegenthaler, U.: 13C/12C isotope ratios in trees are sensitive to relative humidity, Dendrochronologia, 7, 9–13, 1989.

Saurer, M., Siegenthaler, U., and Schweingruber, F.: The climate-carbon isotope relationship in tree rings and the significance of site conditions, Tellus B, 47, 320–330, 1995.

Scafaro, A. P., Fan, Y., Posch, B. C., Garcia, A., Coast, O., and Atkin, O. K.: Responses of leaf respiration to heatwaves, Plant Cell Environ., 44, 2090–2101, https://doi.org/10.1111/pce.14018, 2021.

Schweingruber, F. H., Fritts, H. C., Bräker, O. U., Drew, L. G., and Schär, E.: The X-ray technique as applied to dendroclimatology, Tree-Ring Bulletin, 38, 61–91, 1978.

https://doi.org/10.5194/egusphere-2026-4943
Preprint. Discussion started: 28 September 2026

Shah, S. K., Berkelhammer, M., Li, Q., Mehrotra, N., Thomte, L., Shell, R., Pandey, U., Gaire, N. P., Kathayat, G., and Sinha, A.: Regional tree-ring oxygen isotope deduced summer monsoon drought variability for Kumaun-Gharwal Himalaya, Quaternary Sci. Rev., 301, 107927, https://doi.org/10.1016/j.quascirev.2022.107927, 2023.

Sidor, C. G., Popa, I., Vlad, R., and Cherubini, P.: Different tree-ring responses of Norway spruce to air temperature across an altitudinal gradient in the Eastern Carpathians (Romania), Trees, 29, 985–997, https://doi.org/10.1007/s00468-015-1178-3, 2015.

Solomon, S.: Climate Change 2007: The Physical Science Basis, Cambridge University Press, Cambridge, UK and New York, NY, USA, 2007.

Song, H., Zeng, X., Liu, Y., Björklund, J., Sun, C., Ma, Y., Zhang, Q., Li, P., Wu, X., and Li, Q.: Earlywood and latewood density in pines from northern subtropical China exhibit distinct and robust climate signals, Ecol. Indic., 175, 113575, https://doi.org/10.1016/j.ecolind.2025.113575, https://doi.org/10.1016/j.ecolind.2025.113575, 2025.

Stokes, M. A.: An introduction to tree-ring dating, University of Arizona Press, Tucson, AZ, USA, 1996.

Torrence, C. and Compo, G. P.: A practical guide to wavelet analysis, B. Am. Meteorol. Soc., 79, 61–78, https://doi.org/10.1175/1520-0477(1998)079%3C0061:apgtwa%3E2.0.co;2, 1998.

Touchan, R., Funkhouser, G., Hughes, M. K., and Erkan, N.: Standardized precipitation index reconstructed from Turkish tree-ring widths, Climatic Change, 72, 339–353, https://doi.org/10.1007/s10584-005-5358-9, 2005.

Touchan, R., Akkemik, Ü., Hughes, M. K., and Erkan, N.: May–June precipitation reconstruction of southwestern Anatolia, Turkey during the last 900 years from tree rings, Quaternary Res., 68, 196–202, https://doi.org/10.1016/j.yqres.2007.07.001, 2007.

Verheyden, A., Roggeman, M., Bouillon, S., Elskens, M., Beeckman, H., and Koedam, N.: Comparison between δ13C of α-cellulose and bulk wood in the mangrove tree Rhizophora mucronata: implications for dendrochemistry, Chem. Geol., 219, 275–282, https://doi.org/10.1016/j.chemgeo.2005.02.015, 2005.

Wilson, A. and Grinsted, M.: 12C/13C in cellulose and lignin as palaeothermometers, Nature, 265, 133–135, https://doi.org/10.1038/265133a0, 1977.

Wilson, R. J. and Hopfmueller, M.: Dendrochronological investigations of Norway spruce along an elevational transect in the Bavarian Forest, Germany, Dendrochronologia, 19, 67–79, 2001.

Wilson, R. J., Luckman, B. H., and Esper, J.: A 500 year dendroclimatic reconstruction of spring–summer precipitation from the lower Bavarian Forest region, Germany, Int. J. Climatol., 25, 611–630, https://doi.org/10.1002/joc.1150, 2005.

Wilson, R., Rao, R., Rydval, M., Wood, C., Larsson, L.-Å., and Luckman, B. H.: Blue Intensity for dendroclimatology: The BC blues: A case study from British Columbia, Canada, Holocene, 24, 1428–1438, https://doi.org/10.1177/0959683614544051, 2014.

Wilson, R., Anchukaitis, K., Briffa, K. R., Büntgen, U., Cook, E., D'Arrigo, R., Davi, N., Esper, J., Frank, D., and Gunnarson, B.: Last millennium northern hemisphere summer temperatures from tree rings: Part I: The long term context, Quaternary Sci. Rev., 134, 1–18, https://doi.org/10.1016/j.quascirev.2015.12.005, 2016.

Wilson, R., Anchukaitis, K., Andreu-Hayles, L., Cook, E., D’Arrigo, R., Davi, N., Haberbauer, L., Krusic, P., Luckman, B., and Morimoto, D.: Improved dendroclimatic calibration using blue intensity in the southern Yukon, Holocene, 29, 1817–1830, https://doi.org/10.1177/0959683619862037, 2019.

Wilson, R., Allen, K., Baker, P., Blake, S., Boswijk, G., Buckley, B., Cook, E., D'Arrigo, R., Druckenbrod, D., and Fowler, A.: Evaluating the dendroclimatological potential of blue intensity on multiple conifer species from Australasia, Biogeosciences Discuss., 2021, 1–41, https://doi.org/10.5194/bg-18-6393-2021, 2021.

Zhang, X., Liu, H., and Rademacher, T.: Higher latewood to earlywood ratio increases resistance of radial growth to severe droughts in larch, Sci. Total Environ., 912, 169165, https://doi.org/10.1016/j.scitotenv.2023.169165, https://doi.org/10.1016/j.scitotenv.2023.169165, 2024.

Zheng, Y. and Wilson, R.: Tree ring blue intensity-based August temperature reconstruction for subtropical central China, Forests, 15, 1428, https://doi.org/10.3390/f15081428, 2024.

Zheng, Y., Shen, H., Abernethy, R., and Wilson, R.: Experiments of the efficacy of tree ring blue intensity as a climate proxy in central and western China, Biogeosciences, 20, 3481–3490, https://doi.org/10.5194/bg-20-3481-2023, 2023.